area. It is red to orange in false-color imagery, and corresponds to forests and bushes or to landslide areas. The rivers and creeks show dendritic or sub-parallel patterns; they form deep V-shaped valleys; the drainage density is high. Lineaments appear along 4 directions: NW–SE, NE-SW, N–S and E–W but each of these directions appear in a given zone inside the unit III. The texture is coarse, and the degree of resistance large. The mountain areas corresponding to this unit show mature topographies. This is made up of fractured rocks, which, according to the available geological data, are metamorphic and plutonic rocks of lower Neogene and Paleogene ages.

Geological unit IV: this unit appears sporadically in the high mountains of the central part of the area, north of Daklan. It is light red in color, and corresponds to forests. Rivers are not observed within this unit, and the radial structures that can be seen are difficult to interpret. The texture is very smooth and the resistance is low. This corresponds to Quaternary volcanics that form high dome-shaped mountains, some of which may be interpreted as lava domes.

Geological unit V: this unit occurs as a small patch in the southern part of the analyzed area. It is red to orange in false-color imagery, and corresponds to forests and landslide areas. The rivers have subparallel drainage patterns, and the drainage density is high. The lineaments are not strikingly conspicuous, with NE–SW or NW–SE directions. The texture is relatively smooth, and the resistance is low. This unit shows topography of old age and is interpreted as consisting of metamorphic rocks.

1–4 Stratigraphy

The surveyed area (300 km^2) is underlain by the Dalupirip metamorphics of late cretaceous age (from radiometric dating); the Pugo (mainly volcanics) and Columbus (limestones) formations, both of Paleogene age; the Zigzag formation, composed mainly of lower Miocene volcanics; the Klondyke formation, which consists of Middle Miocene sedimentary rocks; the Rosario formation (Upper Miocene-Pliocene sediments); and the Balatoc plug and Terrace deposits of lower Pleistocene age (Table II–1–2, Fig. II–1–3, Fig. II–1–4).

1–4–1 Dalupirip Schists (Da)

Previous studies: These rocks have been named by Dickerson (1923), who designated the crystalline schists, diorites, slates and cherts as composite basement rocks. Leith (1938) used this formation name for the metamorphic rocks of the basement. Fernandez and Pulanco (1967) did not use any specific name because they considered these rocks as locally metamorphised by the intrusion of so-called "composite dioritic rocks". Oca (1951) and Balce (1979) consider

Table II–1–2 Generalized Stratigraphic Column

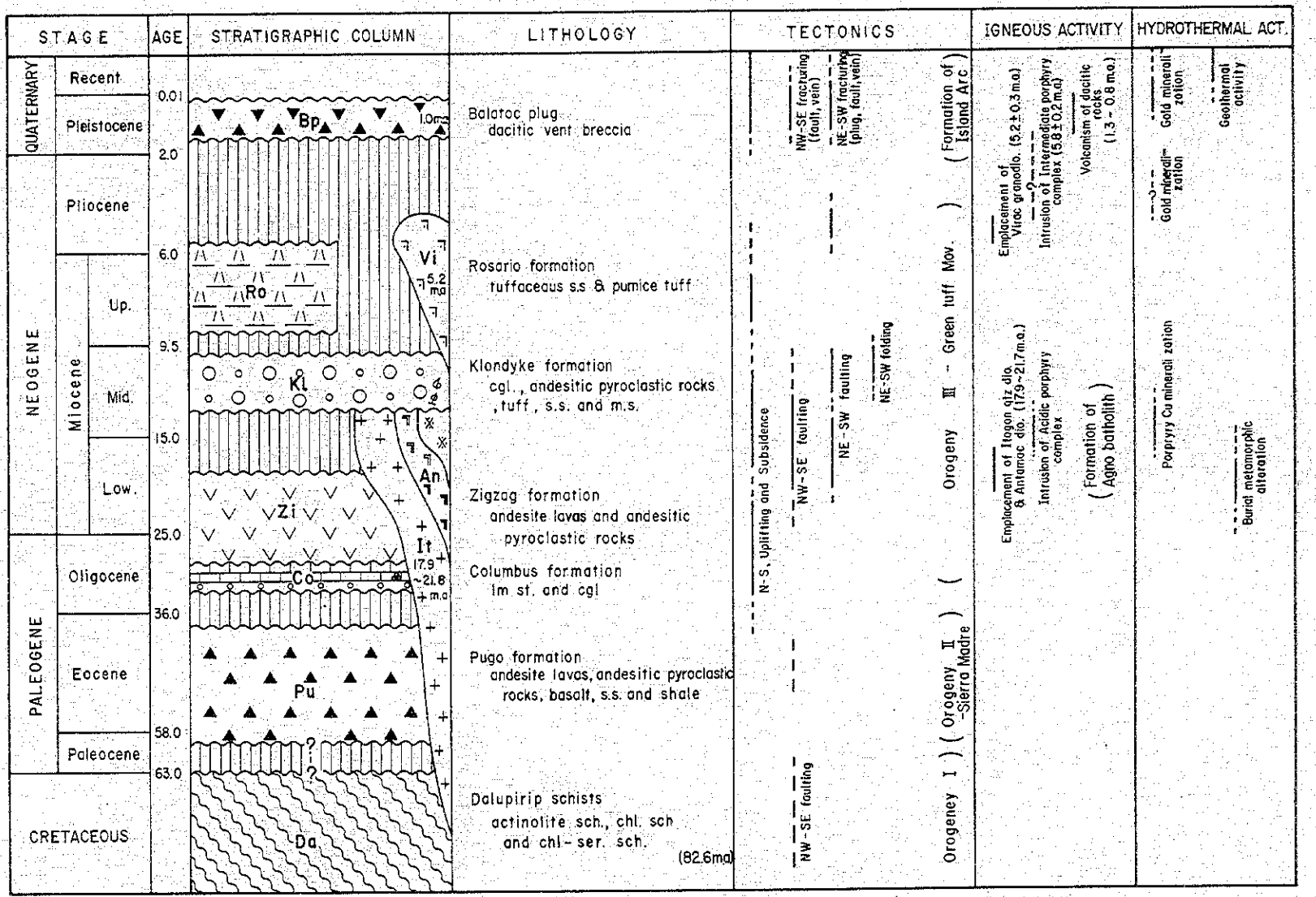

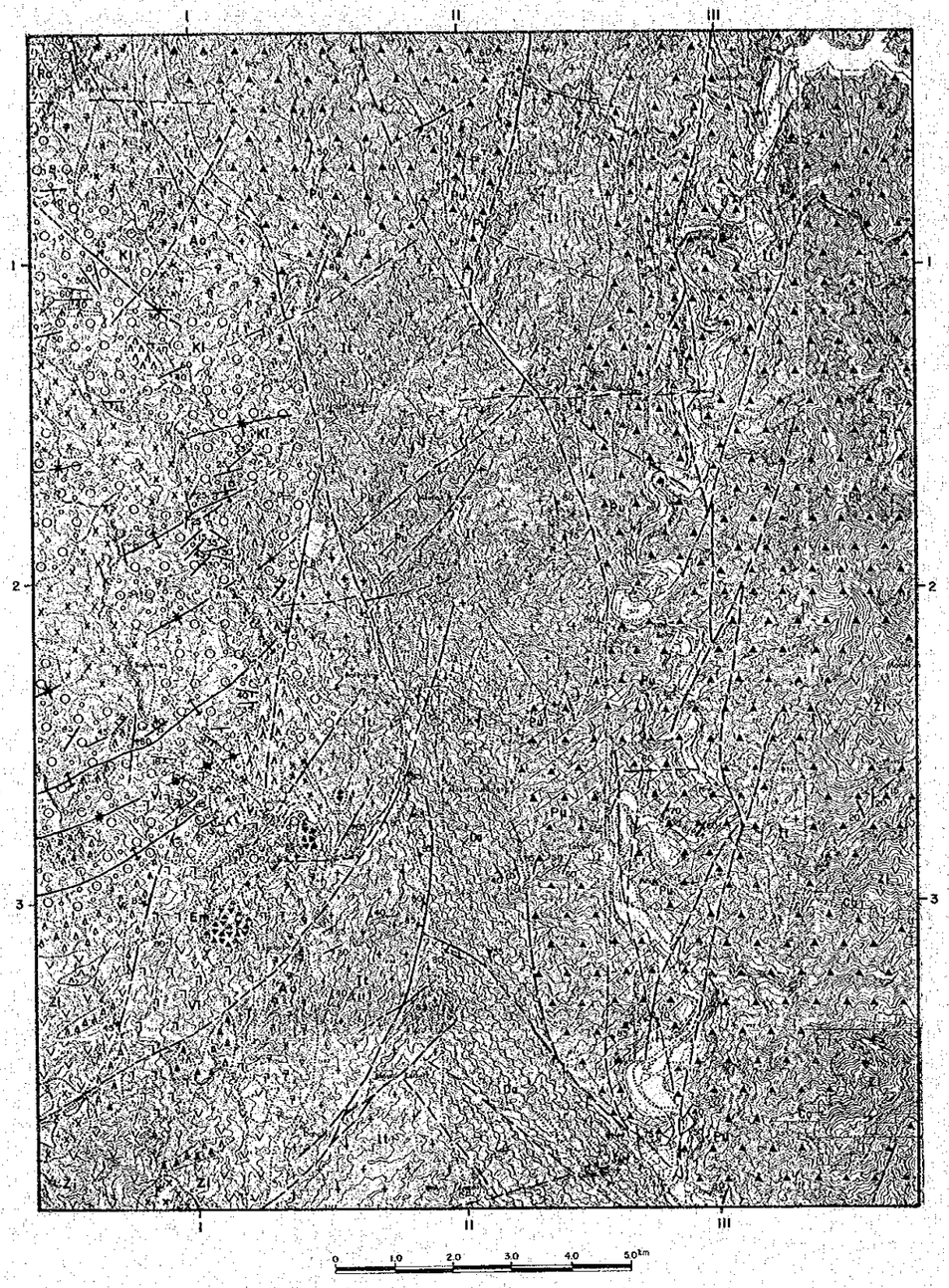

LEGEND

Quaternary
- Pleistocene — Terrace dep. — gravel
- Pleistocene — Balotoc ploy — dacitic pyroclastic r. <0.85±0.12 m.a.>

Tertiary
- Pliocene — Upper — Rosario F. — s.s. & pumice tf.
- Miocene — Middle — Klondyke F. — conglomerate, pyroclastic r., tf, s.s. & m.s.
- Miocene — Lower — Zigzag F. — andesitic pyroclastic r. and andesite
- Oligocene — Columbus F. — lime stone
- Eocene — Pugo F. — metavolcanic r. & metasedimentary r.
- Paleocene

Up Cretaceous — Balupirip sch — sch.

<Intrusive rocks>

- hb mega crstal bearing and porphyry <5.76±0.23 m.a.>
- intermediate volc-plutonic complex (and, and. porphyry and micro diorite bearing hb)
- px. and porphyry
- acidic to intermediate volc-plutonic complex (composed of mainly qtz dio.por, a minor amount of docite porphyry, and qtz diorite, andesite, and porphyry)

Agno batholith
- bio-hb qtz diorite ~ granodiorite(so called virac granodio) [medium grained to fine] <5.20±0.33 m.a.>
- hb diorite, hb gabbroic diorite (cos. grained)
- melanocratic to leucocratic hb qtz diorite <17.0~22.7 m.a.> (cos.grained to medium grained, main body of Agno batholith)

- transition zone (alternative sentech, and meta-volcanics and/or meta-sediment)
- bedding
- schistosity
- foliation
- joint
- fault
- lineament
- operating mine and closed mine
- hot spring
- anticline, syncline

Fig. Ⅱ-1-3 Geological Map

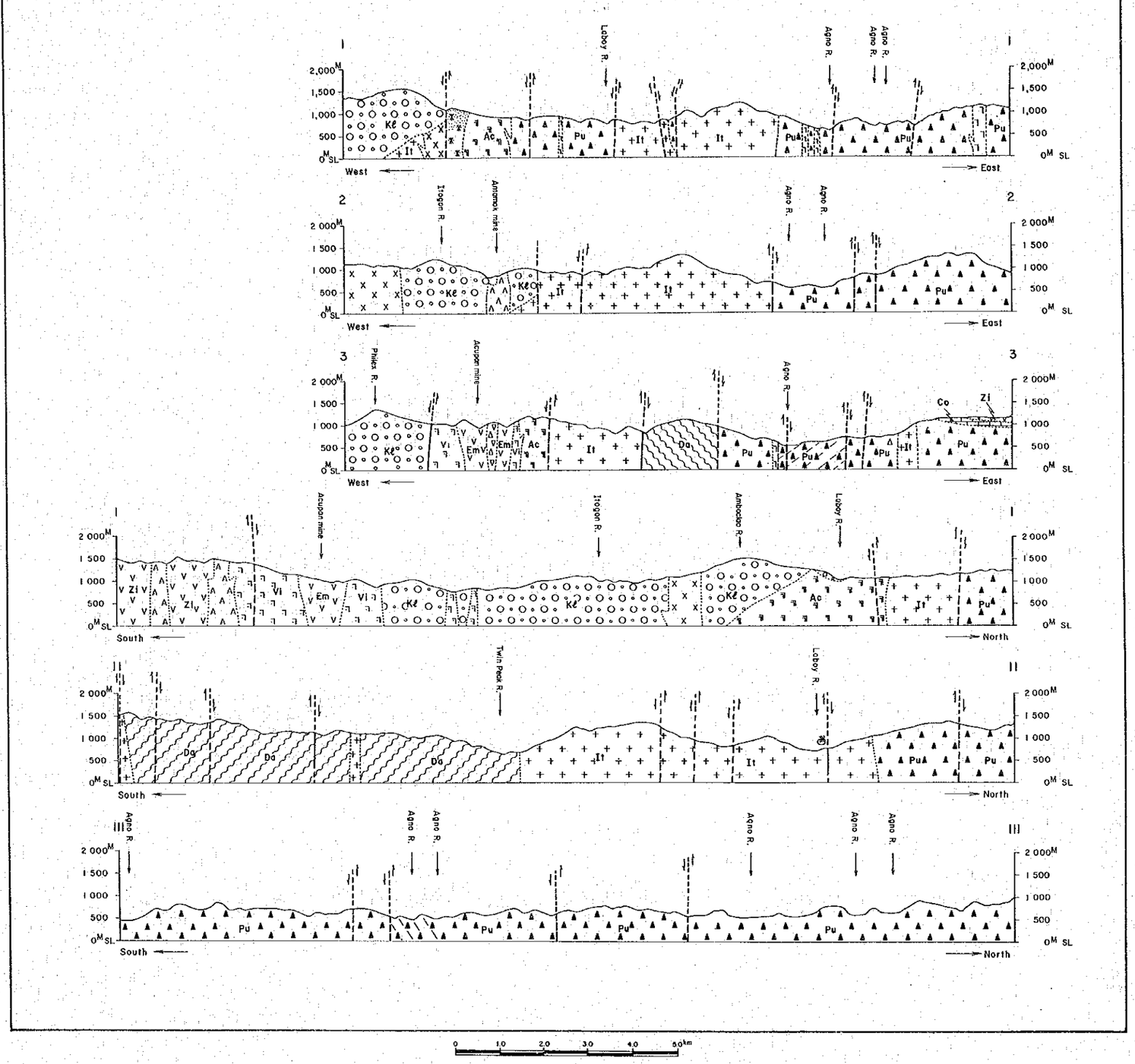

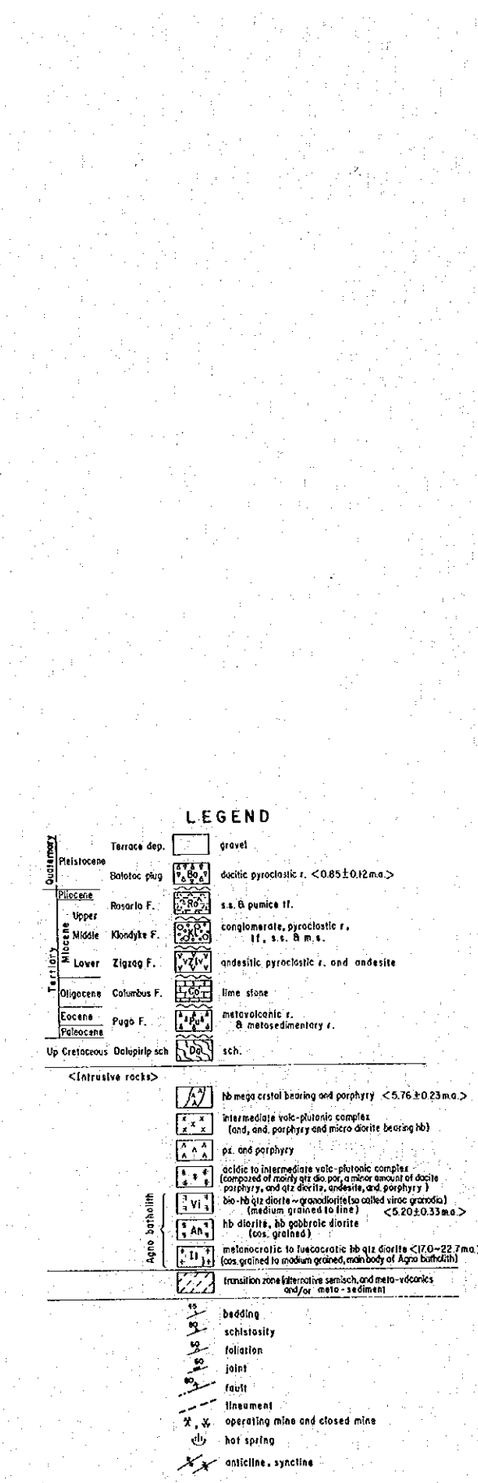

Fig. Ⅱ-1-4 Geological Profile

these rocks transitional to the Pugo formation, which consists of metavolcanics and metasediments. MMAJ-JICA (1976, 1977), on the basis of K-Ar radiometric dating, consider these rocks as having been metamorphosed during late Cretaceous and hence are older than the Pugo formation.

Type locality: Itogon Municipal, along the Itogon-Dalupirip road at Twin River village.

Stratigraphic relations: This formation is in fault contact with the Pugo formation, and is intruded by the Itogon Quartz diorite. Dalupirip metamorphic rocks are found as pebbles in conglomerates of the Klondyke formation, which unconformably overlies the Dalupirip formation.

Thickness: unknown.

Distribution: in a NNW–SSE zone extending from the west of Dalupirip to the village of Twin River.

Lithology and Structure: this formation consists of alternating layers, several of tens cm thick, of dark actinolite schists and light to dark green greenschists. The contact between two layers probably corresponds to the original stratification of the schistose rocks.

The dark actinolite schists are hard and compact, and fine- to medium-grained. The fine-grained facies resemble black schists derived from mudstones.

Among the greenschists may be distinguished, megascopically, dark green (epidote) chlorite schists, green (epidote) sericite – chlorite schists and light green (epidote) chlorite – sericite schists.

The schistosity has a NW–SE to N–S direction and a more or less steep dip to the E or W.

These metamorphic rocks are in fault contact with the Pugo formation on the western side, and are intruded, in the northern and eastern sides, by the Itogon quartz diorite. The Dalupirip metamorphic rocks are found scattered in a NNW direction as xenoliths in the Itogon quartz diorite. Beyond the southern limits of the investigated area, metamorphic rocks (principally amphibolites) with a NE–SE schistosity are distributed in the NW–SE direction. They have fault contact with the Pugo formation on both sides (MMAJ-JICA, 1976).

Observation under the microscope: epidote-chlorite-actinolite schist (Fig. II–1–5). Samples No. A–138, green-schist (according to field observation) located 3 km East of Itogon Municipality. Banded structure appearing clearly under the microscope; porphyroblastic texture. Plagioclase > Quartz > Actinolite > Chlorite ≫ Epidote ≫ Sphene. Two type of plagioclases are observed; (1) coarse-grained (near diameter 0.1 mm, up to 1.8 mm) idiomorphic or hypidiomorphic granular to short prismatic, anorthite-rich grains and (2) fine (±0.03 m/m) xenomorphic grains of albite-rich plagioclase. Quartz forms fine xenomorphic grains (0.03 m/m) showing

undulatory extinction. Actinolite forms fibrous idioblasis, up to 0.5 m/m in length, and is often found interlayered with chlorite. Epidote also shows an idiomorphic habit.

Age: the general schistosity of these metamorphic rocks is discordant with the direction of emplacement of Itogon Quartz diorite and becomes harmomic near the contacts with the quartz diorite. Furthermore, outside the limits of the investigated area, the metamorphic rocks are not in contact with Itogon quartz diorite but with the Pugo formation. Therefore, the Dalupirip metamorphic rocks have no genetic relation with the Itogon quartz diorite, which they predate. Moreover, an amphibolite located at about 8 km south of the survey area gave a K-Ar radiometric age of 80.6 ± 20.6 m.a. (MMAJ-JICA, 1977). The metamorphism is thus considered to have taken place in late Cretaceous (BCI, 1976).

1–4–2 Pugo Formation (Pu)

Previous studies: Peña, (1970) and Peña and Reyes (1970) used this formation name for metavolcanics and metasediments that were called "Pugo Series" by Schafer (1954). The litho-stratigraphy and structure of this formation have been described in detail by MMAJ-JICA (1976, 1977) under the name of Caraballo group. According to these reports, it consists mainly of basaltic and andesitic rocks with associated sediments, folded in the N–S direction. Its age is considered to be Eocene-Miocene on the basis of its relations with intrusive rocks. On the contrary, B.C.I. (1976) and Balce et al. (1978) consider it to be Cretaceous – Oligocene.

Type locality: Road between Laboy Bridge (along Ambuklao Road) and Ambuklao Dam, Itogon, Benguet.

Stratigraphic relations: Unconformably covered by the Columbus formation.

Thickness: unknown.

Distribution: This formation is largely distributed in the N–S direction along Agno River, and northward from the left bank of Laboy River.

Lithology and Structure: The Pugo formation consists principally of dark green to green andesitic and basaltic volcanics associated with thick intercalations of grey to light green sediments and green sediments. These rocks are characterized generally by chloritization, silicification, and hardness.

The andesitic rocks consist of pyroclastic breccias, lapilli tuffs, hyaloclastites and lavas. They are products of a volcanic activity characterized by the extrusion of lavas of basaltic andesite composition. The volume of basaltic rocks, consisting of pyroclastic breccias and lavas is small compared to that of the andesitic rocks. Pillow lavas may be observed on the left side of Agno River, 5 km East of Itogon. The sediments consist of siliceous sandstones, tuffs, conglo-

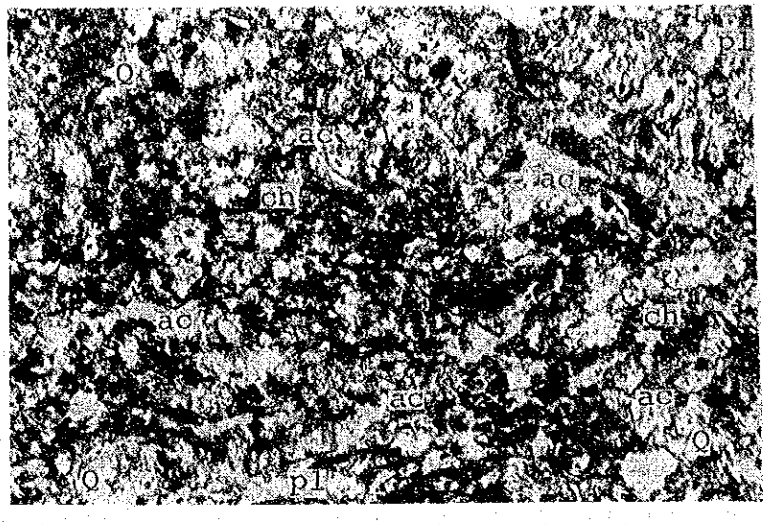

Fig. II−1−5 Microscopic photo of Dalupirip Schist (A-138)
ac; actinolite, ch; chlorite, Q; quartz, pl; plagioclase

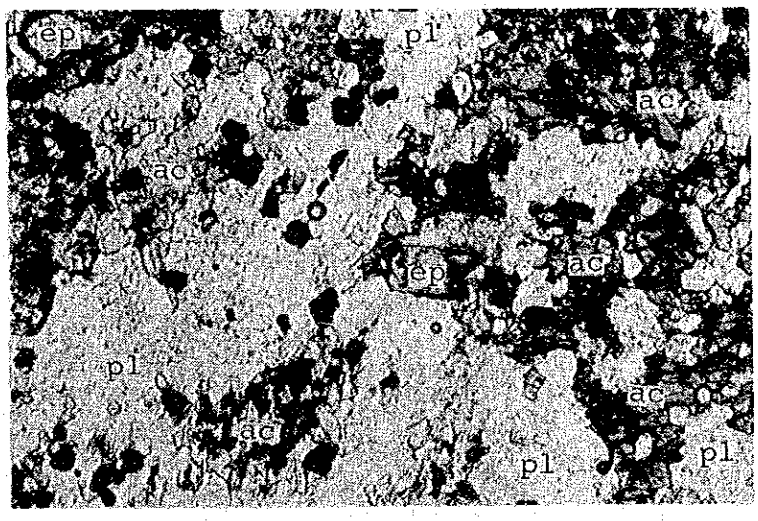

Fig. II−1−6 Microscopic photo of Altered andesite of Zigzag Formation (B-127)
ac; actinolite, pl; plagioclase, epi; epidote

merates and shales. They are chloritized to the same degree as the volcanic rocks. They exhibit alternate stratification with a layer having an average thickness of 0.1 meter. The conglomerates contain fragments of intermediate sizes, some of which are derived from cherts, but those derived from metamorphic rocks were not observed. Paraschists belonging to the Pugo formation are distributed within a narrow N–S zone along Agno River, south of Itogon-Dalupirip road. They are found interlayered with andesitic lavas, and are probably derived from pyroclastic rocks.

With respect to the structure of this formation, the rhythmic banding of the sediments dip more or less gently eastward or westward; this formation is thus folded. However, because of intrusive rocks and faults, it is difficult to trace out continuously the succession of rock types; therefore, the internal stratigraphy of the formation remains unclear.

〈Microscopic photo〉 Sample No.B–127 altered andesite (Fig. II–1–6)

1–4–3 Columbus Formation (Co)

Previous Studies: this formation, named by MMAJ-JICA (1977), is reportedly of Oligocene age on the basis of foraminefera occurrences.

Type locality: upper part of Columbus creek, in the SE of Itogon Municipality.

Stratigraphic relations: this formation lies unconformably on the Pugo formation, and is unconformably overlain by the Zigzag formation.

Thickness: 200 m ±

Distribution: at several high places scattered in the SE part of the area.

Lithology and structure: this formation begins with a basal conglomerate and consists mainly of massive or brecciated white to bluish-white limestones, locally associated with tuffs. This formation has a general N–S direction and is slightly folded.

The conglomerates of the lower part of this formation contain fragments of metavolcanics and metasediments derived from the Pugo formation, which is unconformably covered by the Columbus formation. The stratified layers of the Columbus formation is cut by the Zigzag formation. The latter formation is thus considered to lie unconformably over the Columbus formation.

Age: the following macroforaminiferas were obtained from massive limestone (MMAJ-JICA, 1976):

Spiroclypeus leupoldi van der Vlerk, Nephrolepidina sp., Eulepidina monstrosa Yabe, Amphistegina radiata; they denote an Oligocene age.

1–4–4 Zigzag formation (Zi)

Previous studies: Leith (1938) gave this name to well-stratified sediments occurring in the

upper stream of Bued River, and considered them as middle Miocene in age. Peña (1969) and Peña & Reyes (1970) favor a late Oligocene – middle Miocene age, Balce et al (1978) a late Oligocene – early Miocene age, and Santos (1982) an Oligocene to early Miocene age.

Type locality: Along the upper stream of Bued River, around Zigzag, on Kennon road, Tuba Municipality (outside the limits of the investigated area).

Stratigraphic relations: this formation has been reported as being uncomformably overlain by the Klondyke formation near the type locality of Bued River, which is beyond the limits of the area. The relations between Zigzag and Klondyke can not be observed directly in the area, but fragments derived from Zigzag formation are observed in the Klondyke formation. The Zigzag formation is intruded by several bodies of intrusive rocks, namely: Itogon quartz diorite, Antamok diorite, Virac granodiorite and by quartz diorite porphyry-quartz diorite complexes associated with porphyry copper deposits.

Thickness: 1,400 m±

Distribution: Around the Acupan mine, in the Southwestern part of the area, and in the mountains around Columbus creek, in the Northeastern part.

Lithology and structure: this formation consists of green to dark grey andesitic volcanics and green to light green tuffaceous sediments. One characteristic of this formation is the strong propylitization, which closely resemble those of the so-called "Green tuff region" of Neogene age in North-East Japan. All the colored minerals in the volcanic rocks of this formation have been replaced by alteration minerals, and the mineral morphologies are difficult to recognize. The andesitic lavas occurring in eruptive complexes, as seen around Acupan Mine, have been called Emerald Creek andesite by Schafer (1954) and BCI (1976). The tuffaceous sediments of this formation are characteristically stratified with beds varying in thickness from 0.1 to 10 meter. The fresh parts are green to dark green in color, while the weathered parts show the brown color of the so-called "choco tuffs". The stratification generally strikes in the N–S direction; it is slightly folded.

1–4–5 Klondyke Formation (Kl)

Previous studies; In the first, Leith (1938) used the formation name for the thick pyroclastics and conglomerate exposed in Camp 1 to Camp 3 along the Kennon road. After his work, this formation name has been used for the same formation by Corby et al. (1951), Durkee and Pederson (1961), Balce et al. (1979) and Santos (1982). Peña and Reyes (1971) named Klondyke conglomerate for this formation.

This report uses Klondyke formation to follow the formation name of Corby et al. (1951) et al.

Peña and Reyes (1971) thought that this formation was collated with the Middle ~ Upper Miocene age by the stratigraphic relationships, but the recent studies after Balce et al. (1979) think it to be collated with the Middle Miocene age by the data of fossils.

Type Locality; This type outcrops are exposed in Camp 1 to Camp 3 along Kennon road.

Distribution; This formation is widely occurred in the western central parts in this survey area.

Stratigraphic relations: This formation is overlain by Mirador Limestone in unconformably what is reported in the western side of Trinidad by Peña (1969) et al.

This formation is unconformably overlain on Antamok diorite and a porphyry copper deposit in a northern branching road of the Anbuclao road. In the other parts, the contacts between this formation and others are faults and intrusive relations.

This formation is intruded by Virac granodiorite (K–A) age; 5.20 ± 0.33 Ma), hornblende andesite porphyry (K–Ar age ; 5.76 ± 0.23 Ma) and micro diorite bodies.

Thickness : about 3,000 m

Lithology and Structure : The Klondyke formation consists principally of pale green to dirty gray andesitic pyroclastics and conglomelate associated with sandstone, mudstone and andesite lava.

This formation is characterized by thick volcanic conglomerate and thick conglomerate, and they consist with clasts of plutonic rocks as qtz diorite, tonalite and diorite.

The lithologies are changing from finer materials in the northern parts of the Ambuklao road to coarser materials in the southern parts, and the relationship of lithologies is the interfinger one.

The lowest sequence of this formation is observed that the basal conglomerate is overlain by the alternation of tuff and mudstone in the northern part of the Anbuclao road. The basal conglomerate consists with the angular clasts of qtz diorite porphyry in the 50 cms horizon in thickness over the disconformable contact with green copper bearing qtz diorite porphyry. The upper members on the above mentioned sequence are composed with alternation of conglomerate, sandstone, lapilli tuff, tuff and mudstone with the thickness of about 1,000 ms in the finer materials area. Therefore, the contacts between this formation and the others are observed to be the fault one and the intrusion one in the coarser materials area. The members in the coarser materials area are mainly composed of volcanic breccia, tuff breccia and volcanic conglomerate accompanied with lapilli tuff, conglomerate, tuff, sandstone and mudstone.

The hyaloclastite lava of px-hb andesite, the impression fossil of a bivalva and trace fossils are observed in the upper steam of the Antamok mine.

In generally, the strikes of this formation are trending NW–SE to NE–SW with 10° ~ 60° in dipping, and the beddings are represented as the half basin structure opening to the west side and as gently folded structure with E–W to NE–SW of fold axis and 2 kms to 1.5 kms of wave length.

< Microscopic photo > Sample no. B-6 hornblende andesitic tuff breccia (Fig. II–1–7).

Age : This formation is unconformably overlain on Itogon qtz diorite (K–Ar age ; 21.94 ± 0.93 Ma) and the porphyry copper mineralization, and this formation is intruded by hornblende andesite porphyry (K–Ar age ; 5.76 ± 0.23 Ma) and Virac granodiorite (K–Ar age ; 5.20 ± 0.33 Ma). Balce et al. (1978) and Santos (1982) correlate this formation to be in the Middle Miocene age. Accordingly, the age of this formation is considered the Middle Miocene age.

1–4–6 Balatoc Plug

Previous studies : B.C.I. (Benguet Cooperation Industry, 1970) and Peña (1974) used the name of "Balotoc Plug" for dacitic pyroclastic rocks in which the gold veins of the Acupan mine occur. Therefore, B.C.I. reported the dacitic pyroclastic rocks in the mine occur as diastream-like in vertically.

Type locality : at the Acupan mine and the upper stream of the Itogon bridge.

Stratigraphic relation : This plug is composed of the clasts of Virac granodiorite (K–Ar age ; 5.20 ± 0.33 Ma) and it is intruded by dacite intrusion (Fission track age ; 1.0 Ma).

Distribution : at the Acupan mine and the northeastern parts of the Itogon town.

Thickness : more than 700 ms

Lithology and structure : This rock facies are composed of pale green to light gray dacitic lapilli tuff and tuff breccia. This rocks are consolidated well. The clasts of these pyroclastics consist in granodiorite, hornblende andesite porphyry, hornblende qtz diorite, hornblende diorite, hornblendite and dacite porphyry.

In the Acupan mine, the member of tuff breccia is distributed in the outer zone of Balatoc plug and the member of lapilli tuff is occurred in the inner zone of it. The aboved mentioned evidences might show that Balotoc plug is formed as a eruption vent and collapse of eruption vent in about 1 km of diameter.

Therefore, the same rock facies are distributed with 0.5 kms of diameter at the upper stream of the Itogon bridge and with 0.3 kms of diameter at the northern part of Itogon town. The former plug is named Itogon plug by this survey.

These three plugs align NE–SW trending, and the alignment is parallel to the southeastern margin of the basin for Klondyke formation.

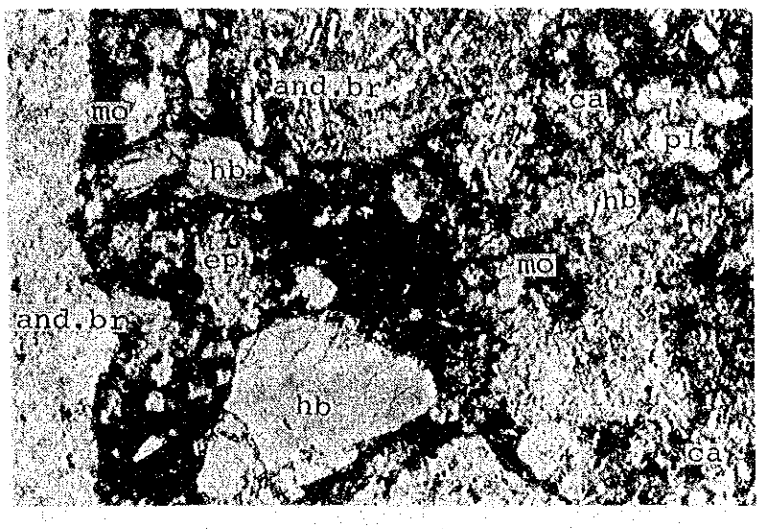

Fig. II−1−7 Microscopic photo of Andesitic tuff breccia of Klondyke Formation (B-6) and br; inclusion of andesite, hb; hornblende, pl; plagioclase, ep; epidote, mo; montomorillorite, ca; calcite

Table II–1–3 Isotopic Age Determination of Fission–Track Method and K-Ar Method

(1)

Fisson Track Age datasheet

Sample NO. : A-208

Locality :

Purpose : Rock Name(Formation) :

Seperated Mineral : Zircon
Etching Condition : Zircon ; KOH-NaOH binary eutectic 200°C-48hr
Mica ; 48% HF , 20°C-30min ,
Standard Glass ; 48% HF , 20°C-15sec ,
U-238 Decay Constant (1/year) : 6.85x10^(-17)
Formula calculated F.T. Age : T=6.12x10^(-8)·P·DS/Di
Thermal Neutron Flux : P=0.830x10^15 ; N= 391 ; D= 1.773x10^5

NO	Spontaneous Track			Induced Track			Ratio of Density (Ds/Di)	F.T.Age (m.y.)
	Count	Cell	Density	Count	Cell	Density		
1	3	250	4.354E+04	296	250	4.296E+06	1.014E-02	0.51
2	9	220	1.484E+05	302	220	4.981E+06	2.980E-02	1.51
3	8	260	1.116E+05	350	260	4.884E+06	2.286E-02	1.16
4	3	200	5.443E+04	316	200	5.733E+06	9.494E-03	0.48
5	12	300	1.451E+05	422	300	5.104E+06	2.844E-02	1.44
6	7	300	8.466E+04	238	300	2.879E+06	2.941E-02	1.49
7	6	200	1.089E+05	258	200	4.681E+06	2.326E-02	1.18
8	11	300	1.330E+05	308	300	3.725E+06	3.571E-02	1.81
9	9	300	1.089E+05	362	300	4.378E+06	2.486E-02	1.26
10	13	240	1.965E+05	324	240	4.898E+06	4.012E-02	2.04
11	4	200	7.257E+04	208	200	3.774E+06	1.923E-02	0.98
12	2	300	2.419E+04	312	300	3.774E+06	6.410E-03	0.33
13	6	200	1.089E+05	248	200	4.499E+06	2.419E-02	1.23
14	2	200	3.628E+04	180	200	3.266E+06	1.111E-02	0.56
15	4	200	7.257E+04	216	200	3.919E+06	1.852E-02	0.94
16	5	300	6.047E+04	280	300	3.387E+06	1.786E-02	0.91
17	10	240	1.512E+05	324	240	4.898E+06	3.086E-02	1.57
18	5	220	8.246E+04	236	220	3.892E+06	2.119E-02	1.08
19	6	220	9.896E+04	194	220	3.200E+06	3.093E-02	1.57
20	4	200	7.257E+04	154	200	2.794E+06	2.597E-02	1.32
21	5	300	6.047E+04	200	300	2.419E+06	2.500E-02	1.27
22	4	200	7.257E+04	110	200	1.996E+06	3.636E-02	1.85
23	6	300	7.257E+04	122	300	1.476E+06	4.918E-02	2.50
24	4	200	7.257E+04	126	200	2.286E+06	3.175E-02	1.61
1*							(1.28)	1.28
2 A	148	5850	9.180E+04	6086	5850	3.775E+06	2.432E-02	1.24
2 B	148	5850	9.180E+04	6086	5850	3.775E+06	2.432E-02	1.24

Age 1* : Mean F.T.ages calculated from each grain age.
2 : F.T.ages calculated tracks and total observed ares.
A : Used only grains which spontaneous tracks were observed.
B : Used all grains.

Fisson Track Age datasheet

Sample NO. : A-210 (1)

Locality :

Purpose : Rock Name(Formation) :

Seperated Mineral : Zircon
Etching Condition : Zircon ; KOH-NaOH binary eutectic 200°C-48hr
Mica ; 48% HF , 20°C-30min ,
Standard Glass ; 48% HF , 20°C-15sec ,
U-238 Decay Constant (1/year) : 6.85x10^(-17)
Formula calculated F.T. Age : T=6.12x10^(-8)·P·DS/DI
Thermal Neutron Flux : P=0.845x10^15 ; N= 398 ; D= 1.805x10^5

NO	Spontaneous Track			Induced Track			Ratio of Density (Ds/Di)	F.T.Age (m.y.)
	Count	Cell	Density	Count	Cell	Density		
1	6	300	7.257E+04	298	300	3.604E+06	2.013E-02	1.04
2	10	300	1.209E+05	372	300	4.499E+06	2.688E-02	1.39
3	0	200	0.000E+00	140	200	2.540E+06	0.000E+00	0.00
4	4	400	3.628E+04	482	400	4.372E+06	8.299E-03	0.43
5	6	400	5.443E+04	346	400	3.139E+06	1.734E-02	0.90
6	3	300	3.628E+04	304	300	3.677E+06	9.868E-03	0.51
7	5	300	6.047E+04	334	300	4.040E+06	1.497E-02	0.77
8	4	300	4.838E+04	338	300	4.088E+06	1.183E-02	0.61
9	4	200	7.257E+04	268	200	4.862E+06	1.493E-02	0.77
10	4	240	6.047E+04	236	240	3.568E+06	1.695E-02	0.88
11	4	220	6.597E+04	218	220	3.595E+06	1.835E-02	0.95
12	3	200	5.443E+04	154	200	2.794E+06	1.948E-02	1.01
13	2	200	3.628E+04	174	200	3.157E+06	1.149E-02	0.59
14	3	300	3.628E+04	210	300	2.540E+06	1.429E-02	0.74
15	2	200	3.628E+04	208	200	3.774E+06	9.615E-03	0.50
16	2	200	3.628E+04	158	200	2.866E+06	1.266E-02	0.65
17	2	200	3.628E+04	194	200	3.520E+06	1.031E-02	0.53
18	8	300	9.676E+04	348	300	4.209E+06	2.299E-02	1.19
19	7	200	1.270E+05	164	200	2.975E+06	4.268E-02	2.21
20	5	400	4.536E+04	290	400	2.631E+06	1.724E-02	0.89
21	6	300	7.257E+04	282	300	3.411E+06	2.128E-02	1.10
22	2	200	3.628E+04	160	200	2.903E+06	1.250E-02	0.65
23	3	300	3.628E+04	276	300	3.338E+06	1.087E-02	0.56
24	1	200	1.814E+04	70	200	1.270E+06	1.429E-02	0.74
1*							(0.85)	0.82
2 A	96	6160	5.655E+04	5884	6160	3.466E+06	1.632E-02	0.84
2 B	96	6360	5.477E+04	6024	6360	3.437E+06	1.594E-02	0.82

Age 1* : Mean F.T.ages calculated from each grain age.
2 : F.T.ages calculated tracks and total observed ares.
A : Used only grains which spontaneous tracks were observed.
B : Used all grains.

Sample NO. : A-210 (2)

Locality :

Purpose : Rock Name(Formation) :

Seperated Mineral : Zircon
Etching Condition : Zircon ; KOH-NaOH binary eutectic 200°C-48hr
Mica ; 48% HF , 20°C-30min ,
Standard Glass ; 48% HF , 20°C-15sec ,
U-238 Decay Constant (1/year) : 6.85x10^(-17)
Formula calculated F.T. Age : T=6.12x10^(-8)·P·DS/DI
Thermal Neutron Flux : P=0.845x10^15 ; N= 398 ; D= 1.805x10^5

NO	Spontaneous Track			Induced Track			Ratio of Density (Ds/Di)	F.T.Age (m.y.)
	Count	Cell	Density	Count	Cell	Density		
1	6	300	7.257E+04	298	300	3.604E+06	2.013E-02	1.04
2	10	300	1.209E+05	372	300	4.499E+06	2.688E-02	1.39
3	DELETED							
4	4	400	3.628E+04	482	400	4.372E+06	8.299E-03	0.43
5	6	400	5.443E+04	346	400	3.139E+06	1.734E-02	0.90
6	3	300	3.628E+04	304	300	3.677E+06	9.868E-03	0.51
7	5	300	6.047E+04	334	300	4.040E+06	1.497E-02	0.77
8	4	300	4.838E+04	338	300	4.088E+06	1.183E-02	0.61
9	4	200	7.257E+04	268	200	4.862E+06	1.493E-02	0.77
10	4	240	6.047E+04	236	240	3.568E+06	1.695E-02	0.88
11	4	220	6.597E+04	218	220	3.595E+06	1.835E-02	0.95
12	3	200	5.443E+04	154	200	2.794E+06	1.948E-02	1.01
13	2	200	3.628E+04	174	200	3.157E+06	1.149E-02	0.59
14	3	300	3.628E+04	210	300	2.540E+06	1.429E-02	0.74
15	2	200	3.628E+04	208	200	3.774E+06	9.615E-03	0.50
16	2	200	3.628E+04	158	200	2.866E+06	1.266E-02	0.65
17	2	200	3.628E+04	194	200	3.520E+06	1.031E-02	0.53
18	8	300	9.676E+04	348	300	4.209E+06	2.299E-02	1.19
19	7	200	1.270E+05	164	200	2.975E+06	4.268E-02	2.21
20	5	400	4.536E+04	290	400	2.631E+06	1.724E-02	0.89
21	6	300	7.257E+04	282	300	3.411E+06	2.128E-02	1.10
22	2	200	3.628E+04	160	200	2.903E+06	1.250E-02	0.65
23	3	300	3.628E+04	276	300	3.338E+06	1.087E-02	0.56
24	1	200	1.814E+04	70	200	1.270E+06	1.429E-02	0.74
1*							(0.85)	0.85
2 A	96	6160	5.655E+04	5884	6160	3.466E+06	1.632E-02	0.84
2 B	96	6160	5.655E+04	5884	6160	3.466E+06	1.632E-02	0.84

Age 1* : Mean F.T.ages calculated from each grain age.
2 : F.T.ages calculated tracks and total observed ares.
A : Used only grains which spontaneous tracks were observed.
B : Used all grains.

Isotopic age determination of K-Ar method (3)

Sample No.	Rock Name	Mineral	K(%)	^{40}Ar rad (scc/g)	^{40}Ar rad/^{40}Ar(%)	Age (Ma)
A-202	Tonalite	hornblende	0.39	3.3154×10^{-7}	45.83	21.74 ± 0.93
A-206	Amphibole schist	actinolite	0.10	3.0961×10^{-8}	6.22	7.95 ± 2.73
B-157	Granodiorite	hornblende	2.29	4.6327×10^{-7}	30.38	5.20 ± 0.33
B- 09	Hb andesite porphyry	hornblende	0.84	1.8832×10^{-7}	50.73	5.76 ± 0.23

$\lambda e = 0.581 \times 10^{-10}/Y$, $2\beta = 4.962 \times 10^{-10}/Y$, $40K/K = 0.01167$ atm %

Age : The rock facies look that the age of this plug is the Neogene age. Although, the dacite clast in the smallest plug is determined 0.82 ~ 0.84 Ma and the dacite intrusion intruded in Balotoc Plug is determined 1.0 Ma by the fission track method. Accordingly, the age of plugs are presumed to be the Pleistocene age.

1–5 Geological Structure

Geological structure of the investigation area is emphasized by a N–S trending block with minor dislocation caused by NE–SW and NW–SE fractures and is parallel to the general trend of northern Luzon Island. (Fig. II–1–8)

The N–S trending block is uplifted at the central part of the survey area and is accompanied by two subsided zones on both sides of it. Geology of the central uplifted zone is comprised of Dalupirip metamorphic rocks, Itogon quartz diorite, Antamok diorite and Pugo formation. Likewise, that of the eastern and the western subsided zones are comprised of Pugo formation, Colombus formation overlying the Pugo formation, and Zigzag formation (the former); and of Zigzag formation, Virac granodiorite and Klondyke formation (the latter). At the boundary between the central uplifted and the eastern subsided zone are the dyke swarms of quartz diorite within Pugo formation at a few-meter interval, which occur at the northern part of the survey area, and chloritized zones intercalated within Pugo formation at the southern part of the survey area.

The uplifted zone extends along Agno River to the north, and according to the Landsat image it would reach the western uplifted zone of the Bugius district. However both NW–SE trending scistosities within Dalupirip metamorphic rocks and N–S to NNW–SSE trending holiations within Itogon quartz diorite are accordant with the general trend of the central uplifted zone.

At the eastern subsided zone, Columbus and Zigzag formations overlying the Pugo formation are exposed on the ridges almost horizontally. This same structure is also seen at Doklan area where Zigzag formation spreads more widely and Pugo formation does not occur any more. This eastern subsided zone extends to the central subsided zone of the Bugius district. The western subsided zone is geologically composed of Klondyke formation which is younger than the Zigzag formation, and this basin is structurally open to the west.

Fractures are concentrated at the periphery of the central uplifted zone. Especially, the fault structures of NW–SE, NE–SW, and NW–SE systems are prominent at the southeastern, northeastern, and the northwestern regions, respectively.

The fault structure running from north to south at the eastern limb of the central uplifted zone controls the eruption of the hot springs of Laboy and Dalupirip. Likewise, Klondyke hot spring is located on the southwestern extension of the hot spring alignment of Itogon-Acupan mine. The NE–SW trending geological structure around the Acupan-Itogon area is described as follows. First, the alignment of 1-km diameter Balatoc plug, 0.5-km diameter Itogon plug, and 0.25-km diameter plug at northeast of Itogon plug shows the lineaments of the NE–SW trending. Secondly, the southern end of the semi-basin structure formed by the deposition of Klondyke formation has NE–SW trend, and the general strike of ore veins at the Acupan and the Itogon mines also shows this same trend. (Fig. II–1–8) Considering the ages of Klondyke formation, Virac granodiorite and Balatoc plug, which are middle Miocene, Pliocene and Pleistocene, respectively, this NE–SW trending structure has been active to pour hot springs since at least middle Miocene age. But concerning about the areal extent, this structure seems to be confined within an desite of Zigzag formation, Virac granodiorite, and Antamok granodiorite as the ore veins at the Acupan and the Itogon mines do not occur within the Itogon granodiorite. And this indicates that the fractures which make paths for the circulation of geothermal aquifer do not occur within Itogon granodiorite.

1–6 Igneous Activity

The igneous rocks observed in the area include basic to acidic volcanics and intrusive rocks. The stages of igneous activity in chromological order are: (1) pre-tertiary submarine volcanic activity that gave rise to basalts and andesites metamorphosed in late Cretaceous age to actinolite and chlorite schists; (2) submarine volcanic activity, represented by the basalts and andesites that constituted the Paleogene Pugo formation; (3) submarine volcanic activity that produced the andesites of Upper Oligocene – Lower Miocene Zigzag formation; (4) Middle Neogene intrusion of Itogon Quartz diorite and Antamok diorite; (5) Middle Miocene intrusion of quartz diorite porphyry – quartz diorite complexes; (6) submarine volcanic activity showed by small amounts of andesitic material in the Middle Miocene Klondyke formation; (7) late Neogene (Pilocene) intrusion of Virac granodiorite and andesite porphyry – andesite porphyry complexes; and (8) Pleistocene activity that produced the quartz andesite pyroclastic rocks of Balatoc plug and quartz andesite dykes.

1–6–1 Intrusive Rocks

1) Itogon Quartz Diorite (It)

This quartz diorite body was hitherto included, together with Virac granodiorite and

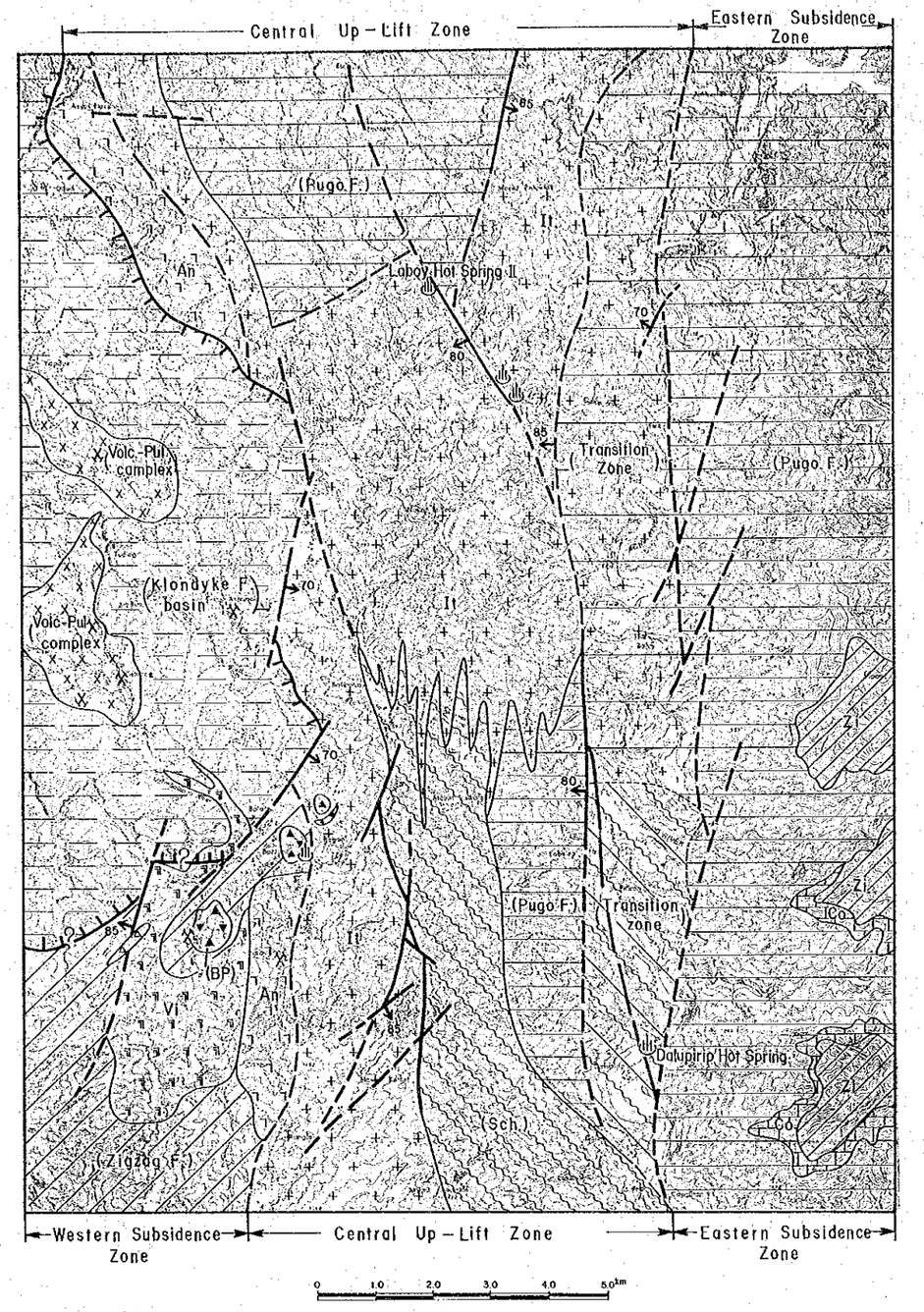

LEGEND

- Fault I
- Fault II
- Unconformable margin of Klondyke F. basin
- Hot spring
- Mine (operating & closed)
- Balaloc pulag (1.0 m.a. ±)
- Klondyke formation
- Zigzag formation
- Columbus formation
- Pugo formation
- Dalupirip schist (82 m.a. ±)
- Virac granodiorite (5.2 m.a.)
- Antamoc granodiorite
- Itogon qtz diorite (17.9~21.7 m.a.)
- Transition zone (Pugo f. to Itogon qtz diorite)
- Transition zone (Alternation of semi-schist and non metamorphosed Pugo f.)

Fig. Ⅱ-1-8 Tectonic Map

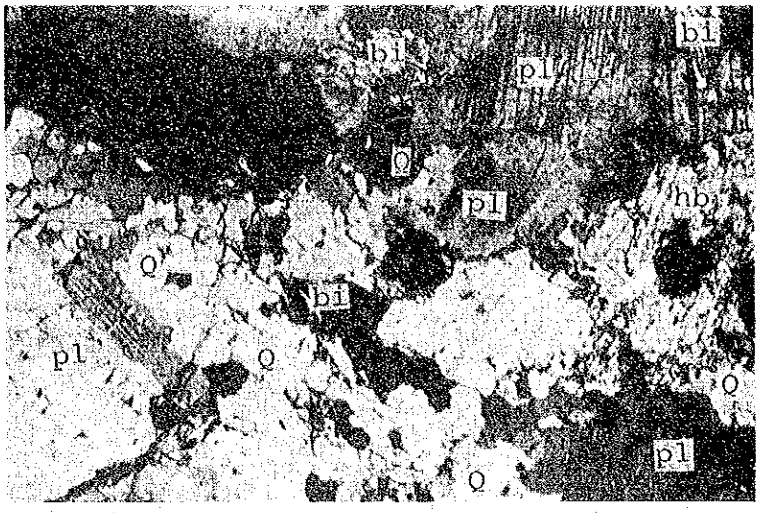

Fig. II–1–9 Microscopic photo of Itogon quartz diorite (A-174)
Q; quartz, pl; plagioclase, hb; hornblende, bi; biotite

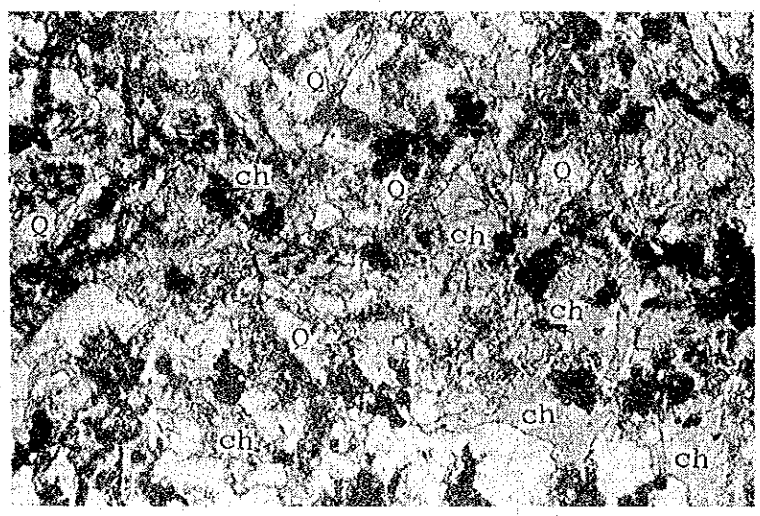

Fig. II–1–10 Microscopic photo of Antamok diorite (A-14)
ch; chlorite, Q; quartz (secondary)

Antamok diorite, in the so-called Agno Batholith (Peña 1969). It extends northward from the south of Itogon, widens in the vicinity of Ambuklao Road and ramifies in the NE and NW directions.

The rocks are leucocratic, generally massive and locally foliated. The texture is medium-grained holocrystalline. The constituent minerals are hornblende and biotite (hb > bi), plagioclase and quartz (PL > Q). This body consists of quartz diorite with a color index around 15≪ (quartz diorite ≫ tonalite). Characteristically, this body is associated with local and weak copper mineralizations.

Tonalite occurs principally in the vicinity of Ambuklao Road, where the Itogon body is wider; a tonalite sample (A-202) taken along this road yielded, by K-Ar radiometric method, an age of 21.74 m.a. (end of early Miocene). On the other hand, the quartz diorite (Fig. II–1–9) forms a belt on the western side of Itogon body, and a sample taken near Itogon yielded a K-Ar age of 17.9 ± 0.9 m.y. (early Middle Miocene).

Itogon quartz diorite intrudes the Zigzag formation and is unconformably covered by Klondyke formation. This body was formed by intrusion of biotite hornblende tonalite followed biotite hornblende quartz diorite from the end of early Miocene to the beginning of Middle Miocene. A central elevated zone was formed by the intrusion of this body.

In the vicinity of Itogon, gold precipitation from high temperature geothermal fluids does not occur within the quartz diorite due to its impermeability to hot water circulation.

2) Antamok Diorite (An) : (Fig. II–1–10)

This diorite, named by Schafer (1954), is the first body to have intruded the main bluk of Agno Batholith. It occurs in the vicinity of Itogon mine and as a zone elongated in the NW–SE or N–S direction on the right side of the upstream of Laboy River.

These rocks are melanocratic, massive with a coarse-to medium-grained holocrystalline texture. They include hornblende diorite (±biotite, ±quartz) and hornblende gabbro (±biotite, ±quartz).

This body intrudes the Zigzag formation and is unconformably covered by the Klondyke formation. The relation of this body with the Itogon body cannot be directly observed, however, these two bodies are considered to form a plutonic series because the ferromagnesian mineral assemblage and the color index of Antamok rocks do not differ very much from that of the basic rocks of Itogon (MMAJ-JICA, 1977).

However, the occurrence of gold veins within this body in Itogon mine shows that there exist, or once existed, in this body, fissure systems that are favorable to geothermal fluid circu-

lation. It is therefore necessary to further investigate the relations between Antamok and Itogon bodies.

3) Quartz diorite porphyry – quartz diorite complexes: (Fig. II–1–11)

These complexes occur as two stocks, 2 km in diameter, in the SW of Acupan mine, and in the upper part of Laboy river.

The constituent rocks are leucocratic, with a fine-grained holocrystalline texture. These rocks are hornblende quartz diorites and quartz diorite porphyries (±biotite). They are characteristically sericitized, and are associated with porphyry copper deposits and related gold mineralization.

This body intrudes the Zigzag formation and Antamok diorite, and is unconformably overlain by the Klondyke formation. It is considered therefore to have intruded 15 m.y. ago (Middle Miocene).

4) Virac granodiorite : (Fig. II–1–12)

The Virac granodiorite, together with the Itogon quartz diorite and Antamok diorite, is a member of the Agno Batholith. It is distributed, in a horseshoe shape, around Acupan mine.

The rock is slightly gray, leucocratic and massive, with a medium-grained, equant, holocrystalline texture. It contains augite, biotite and hornblende, plagioclase, orthoclase, and a small amount of quartz. A special feature of this granodiorite is that it contains numerous xenoliths of fine-grained gabbro.

This granodiorite is intrusive in the Klondyke formation and is subsequently intruded by Balatoc plug. A radiometric age of 5.2 m.y. (Early Pliocene) has been obtained by K-Ar method.

The Virac granodiorite constitutes the host rock of the gold-bearing veins of Acupan Mine, and contains NE–SW fissures where hydrothermal fluids circulate. A part of Acupan Mine hot waters also springs along gold-bearing veins located in this body.

5) Andesitic Porphyry – Diorite porphyry complex

This complex consists of andesite and diorite porphyries. It is located in the vicinity of Baco-Kelly Mine and Baguio gold mine. It constitutes the host rocks of these mines.

6) Dykes of andesite:

These dykes occur on the western flank of Balatoc plug, which they intrude. They represent the most recent volcanic event in the area.

They consist of gray, massive and compact hornblende-quartz andesites. The rocks of these dykes have not yet been observed in the vicinity of the Acupan Mine beneath the western slope of the Balatoc plug. Therefore, their relationship to the gold-bearing veins of the Acupan

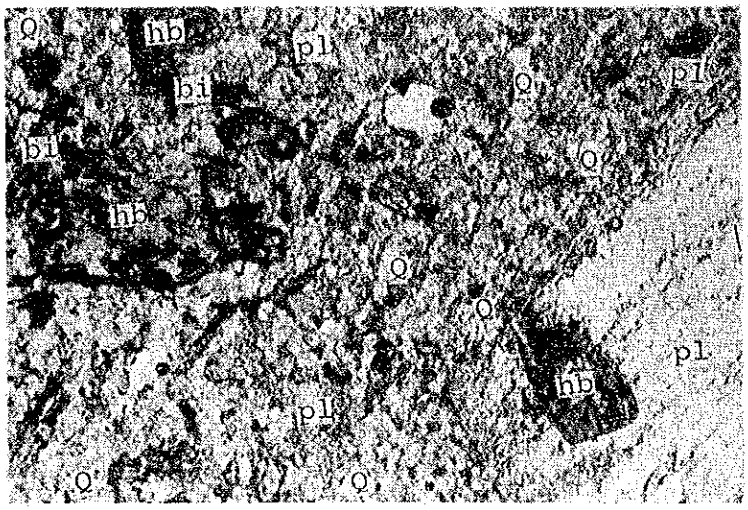

Fig. II–1–11 Microscopic photo of Quartz diorite porphyry (B-125)

Q; quartz, pl; plagioclase, hb; hornblende, bi; biotite

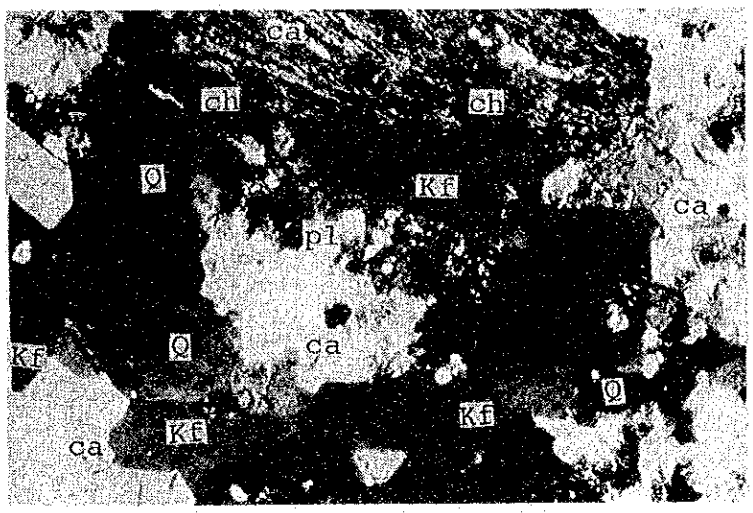

Fig. II–1–12 Microscopic photo of Virac granodiorite (B-39)

Q; quartz, pl; plagioclase, kf; k-feldspar, ch; chlorite, ca; calcite

Table II–1–4 Microscopic Observation

Sample No.	Rock Name	Formation Name or Member Name	Texture	Phenocrysts									Groundmasses										Lithic fragments				Secondary Minerals													
				Q	k-f	Pl	Bi	Ho	Au	Hy	Ol	Op	Q	Si	k-f	Pl	Bi	Ho	Cpx	Opx	Ol	Op	Gl	Ba	An	Da	Tf	Q	Si	Cc	Ser	Mon	Sap	Chl	Kao	Act	Epi	Op	Zeo	Ab	Al
A – 14	quartz-gabbro	Antamok diorite	subophitic			• (An 60%)							◎			◎	○																◎			○	○			
24	cataclastic quartz-diorite	Itogon quartz-diorite	cataclastic				•																				◎								○	◎				
36	chlorite-actinolite-green schist	Dalupirip schist	schistose					◎※																			○								○				○	
44	hornblende tonalite	Itogone quartz-diorite	cataclastic					◎→																					○	○					○				○	
49	mylonite	Pugo formation	mylonitic			•		○※																			○		◎	•			○		•				○	
61	andesite porphyry	dyke	intersertal or porphyritic			◎						•				◎						○							◎					◎						◎	
73	biotite-hornblende granodiorite	Klondyke formation	holocrystalline equigranular (partly cataclastic)	◎	○	◎	○	○※																					•		•		○			•			○	
92	chlorite-actinolite schist	Pugo formation	mylonitic or porphyroblastic	○		○		○※																			○						•		○		○		○	
96	altered andesite	Pugo formation	porphyritic					• ※																			◎			•			•			○				
100	micro-hornblende dolerite	dyke	ophitic			◎		◎※																											○	•				
112	lapilli tuff	Klondyke formation	pyroclastic													◎		◎	○			○	◎		○															
113	biotite-hornblende granodiorite	Itogon quartz-diorite	horocrystalline equigranular (partly cataclastic)	◎	•	◎	○	◎				○															○				•	•	○							
115	hornblende-andesite porphyry	dyke	porphyritic trachytic			•		◎※				○				◎						○					•		•							•	○			
123	altered andesite	Pugo formation	cataclastic	◎		◎																					◎			○			○			○			○	
126	hornblende-gabbro	dyke	ophitic (mainly cataclastic)			◎		◎※				•																					•		◎	•				
127	micro-hornblende-gabbro	dyke	ophitic (partly cataclastic)			◎		○※				•																					•		◎	•				
131	chlorite-epidote-actinolite-green schisto	Pugo formation	schistose																								•						○		◎	•	•		◎	
138	chlorite-actinolite-green schisto	Dalupirip schist	schistose																											○			◎		○	○	○		○	
141	altered basalt	Pugo formation	ophitic					◎※																			◎					•	•		•	○	•		•	
150	biotite-hornblende-tonalite	Itogon quartz-diorite	equigranular	◎	○	◎	•	○?																							•		•	○			○			
158	micro-hornblende-gabbro	dyke	ophitic			○			○			○				◎												○									○				
160	crystal tuff	Klondyke formation	pyroclastic										◎										◎			○+														
174	biotite-hornblende-tonalite	Itogon quartz-diorite	granular	◎		◎	○	◎※				•															○					○	○							
183	biotite-hornblende-tonalite	stock	porphyritic, holocrystalline			◎	○	○	○?			○																						○			○	○			
190	pyroxene dolerite	dyke	ophitic			○			◎			○				◎															○			◎			○	○			
B – 06	hornblende-augite-andesitic tuff breccia	Klondyke formation	pyroclastic																														•							
14	altered basalt	Pugo formation	ophitic					◎※																			◎						•		◎	○	○		◎	
17	chlorite-actinolite-green schist	Dalupirip schist	schistose			○																					○		○		▪		○		•	○			○	
25	hornblende-andesite	dyke	intersertal			◎		○?								◎													◎	○	○			◎				○		○	
29	lapilli tuff	Klondyke formation	pyroclastic													◎		○?				○					○		◎	◎	◎					○	○		○	
34	andesitic fine tuff	do	pyroclastic													◎											◎					•	◎			•	○		○	
37	micro-hornblende-diorite	stock	granular ~ subophitic			◎		◎×				○																					•							
39	biotite-hornblende granodiorite	Virac granodiorite	granular ~ subophitic	◎	•	○	○	○																			○		○	○		•	○							
41	hornblende-gabbro	dyke	granular and porphyritic			◎		◎※																			○		○	•		○	◎			○				
43	actinolite-chlorite-green schist	Pugo formation	schistose																										○				◎	○	◎			○	
45	biotite-hornblende-tonalite	Itogon quartz-diorite	horocrystalline granular	◎	•	◎	○	◎				•																	•				○			•				
46	biotite-dacitic-crystal tuff	Klondyke formation	pyroclastic													◎	○										○		◎	•	○	•	◎				•	•		
51	hornblende tonalite	Itogon quartz-diorite	equigranular	○		◎		◎※				○																	•			•	○			○				
54	biotite-hornblende granodiorite	do	equigranular	◎	○	◎	○	◎				•																	○			•	○			○	•			
69	biotite-dacite	dyke	porphyritic	○			○?																				◎		○	○			◎			◎		○		
80	biotite-hornblende-granodiorite	Itogon quartz-diorite	horocrystalline equigranular	◎	○	○	○	◎※																							○		•	○						
82	actinolite schist	Dalupirip schist	schistose													○											◎		•				○		◎	•	•			
96	hornblende andesite porphyry	dyke	porphyritic			◎		○?				○																	•				◎			○				
97	hornblende-bearing crystal tuff	Klondyke formation	pyroclastic										○			◎		• ?									○		○				•		◎			•		
99	biotite-hornblende-lapilli tuff	do	pyroclastic										◎			•							○	○	◎		○	◎					○		○	◎			•	
117	biotite-hornblende-diorite	Itogon quartz-diorite	granular weakly cataclastic	◎	• ?	○	○	○※																																
123	hornblende diorite porphyry	dyke	porphyritic			◎	•	◎※					◎			○													•	•		•	○							
125	hornblende-biotite-quartz diorite porphyry	stock	horocrystalline porphyritic			◎	○※	◎※					◎			◎	○															•	○						
127	altered andesite	Zigzag formation	(altered)	◎		◎		◎※																				•					•		○	◎	○			
132	altered andesite	Pugo formation	(altered)																								◎	•					○		◎	○	○		○	
136	hornblende-diorite porphyry	stock	horocrystalline	○		◎	•	◎※																										○			○				
139	hornblende-dolerite (micro gabbro?)	dyke	ophitic			◎		○					◎			◎		◎				○											•	◎		○	○	•			
142	augite-dolerite	dyke	ophitic			◎		○?	◎				◎						◎			◎									○					○	•			
145	lapilli tuff	Klondyke formation	pyroclastic																								◎			◎									
153	biotite-granodiorite	Itogon quartz-diorite	horocrystalline equigranular	◎	○	○	◎				•																			○		•	◎			○				

◎: abandant ○: common •: rare ※: green ×: yellow green ∗: brown green

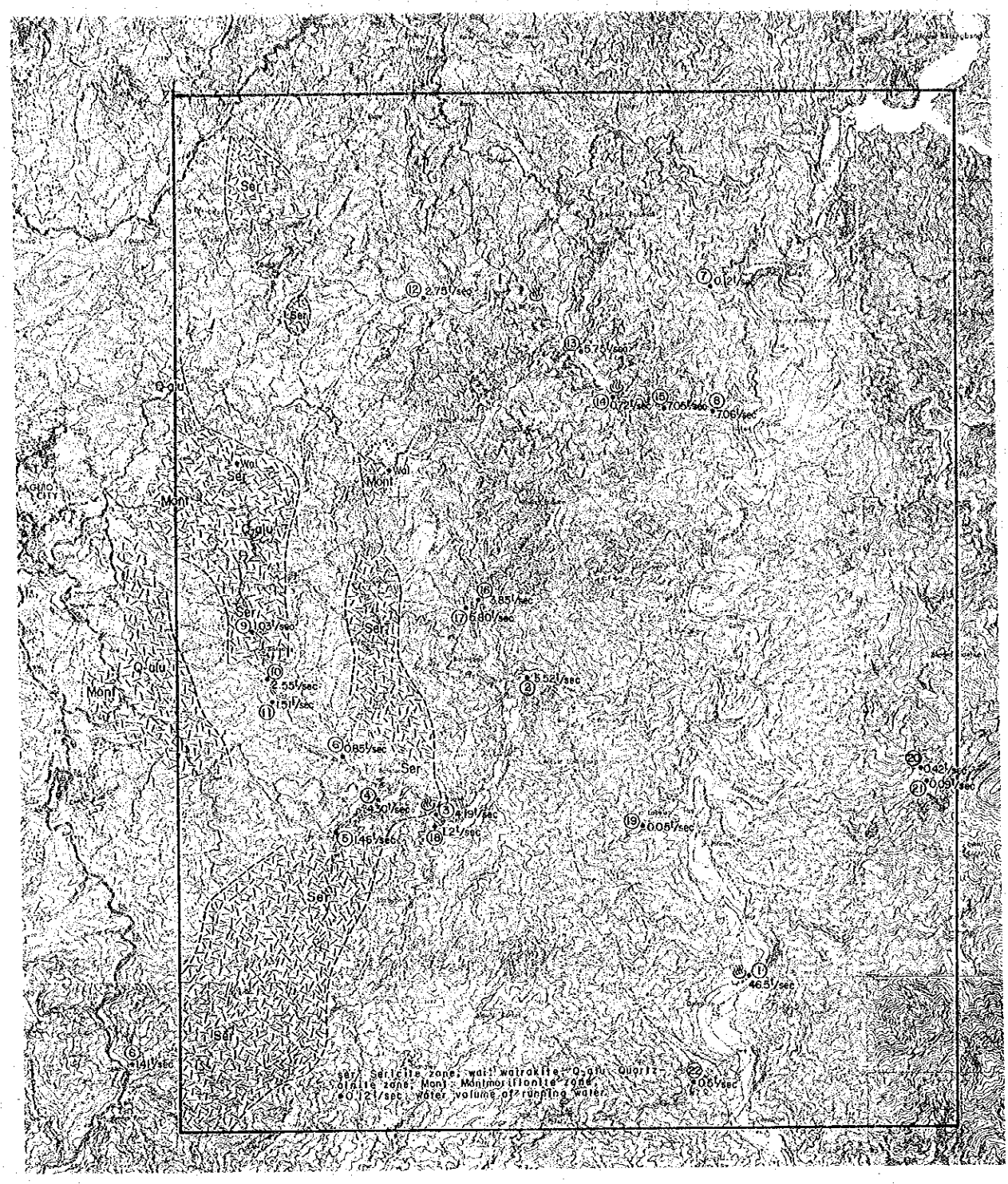

Fig. Ⅱ-1-13 Distribution of Alteration Zone and Volume of Running Water

Table II–1–5 X-Ray Diffraction

Sample No.	Clay minerals							Zeorite minerals					Silica minerals			Carbonate minerals			Sulfate minerals			the others		
	montmorillonite	chlorite	sericite	sericite/montmorillonite (ser. > mont.)	sericite/montmorillonite (ser. < mont.)	kaoline	pyrophyllite	analcime	clinoptilolite	mordenite	loamontite	wairakite	α-cristobalite	tridymite	quartz	calcite	dolomite	rhodonite	alunite	gypsum	anhydrite	pyrite	hematite	epidote
A – 12	◎	○			○			○							△	△						△		
A – 16		◎		○											△	△						△		
A – 20		◎														○								
A – 42	△	◎		○					△							△								
A – 44		◎	○	△											△							△		
A – 52		◎													△							△		
A – 56	△	◎		△				△								○						○		
A – 72	○	○		△											△									
A – 79		○		△												△								
A – 82		◎						△																
A – 83	○	◎													△	△								
A – 85		◎		△												△								
A – 88	○	◎						△								△						△		
A – 98	○	○		○											△									△
A – 103		◎													○	△						△		
A – 104		◎	○	△																				
A – 105		○	△	△				△							○									
A – 108		△				○									△									
A – 113		○	△	△						△					△							△		△
A – 121		◎																						
A – 123			◎	◎																		△		
A – 143	△	◎		△												◎								
A – 145		◎		△																		△		
A – 148	△	◎																						
A – 152		◎	○																					
A – 154	◎	○	◎	△				△								△						△		
A – 156	△	◎																						
A – 167		◎	○								△													
A – 168	◎	○	△												○									△
A – 173		◎	○												◎									
B – 31		△				○									◎									
B – 32		○				△									△									
B – 35		◎																						
B – 38				△						○						○								○
B – 40		◎								△						△								
B – 43		◎								△														
B – 46	○		◎	○																				
B – 47		○	◎	△																				
B – 48			◎	◎																				
B – 49		◎		△												◎								
B – 50		◎		△												◎								
B – 57		◎								△						△								
B – 59	◎					◎										◎								
B – 60																								
B – 61	○	○	○	△												○								
B – 62	◎	○		△																				
B – 69		◎	○	△																				
B – 70	◎	○	◎	◎																				
B – 73	◎	△						○		△												△		
B – 74	◎	△						○														△		
B – 77	◎	○	△								△					○								
B – 79		◎								△					△	△						△		
B – 85		△								△												△		
B – 86	△	◎		△											△							△		
B – 89		△	○													○	△							
B – 90		◎	△													○	○					△		
B – 93		◎	△									△												△
B – 95	△	◎											◎				△					△		
B – 98		○															◎							
B – 100		◎															◎							
B – 104	○	◎					△										○					△		
B – 106		◎																						
B – 108		◎	○																					
B – 110	△	◎														△						△		
B – 111	△	◎																				△		
B – 120		◎														○						△		
B – 121		◎																				△		
B – 126	○	◎	○													◎						△		
B – 128		◎	○													△						△		
B – 132		○								△						△						△		
B – 136	△	◎				△																		
B – 139		◎																						
B – 144						◎	◎			△	△				△									
B – 145							◎								○							○		
B – 146	◎		△		○	○									○									
B – 148		○													△									
B – 149	◎	◎								○		◎			△	△								◎
B – 150	◎	○										△			△							△		
B – 151		◎	○												○									
B – 152		◎																						
B – 154	○	◎										△				△								
B – 155	○	◎				△						○			○	○								
B – 156	○	△					◎								○	◎								
B – 157	◎					△									○									

Mine is not known. Fission track dating of one dyke sample (A-208) yielded and age of 1.28 ± 0.17 m.y. This age is 400,000 years older than the age of an andesitic element found in a small plug 3.5 km NE of Balatoc plug. However, as the dykes cut pyroclastic rocks of Balatoc plug that are much similar to this small plug, their age is considered to be approximately the same as the age of formation of the plug.

As these dikes are located near Acupan Mine, and hence represent the younger volcanic rocks of the region, they are considered to be genetically related with the present geothermal activity of the Acupan-Itogon area.

1–7 Reconnaissance of Geothermal Indications

In the studied area, indices of geothermal activity are found in the zones where hot spring waters originate from, namely: (1) in underground workings of the Acupan Mine, (2) near Itogon bridge and (3) at Dalupirip. Other zones of strong alteration are known, but it is not clear whether they are related to the present geothermal activity, or to the gold mineralization. Three new occurrences of hot spring waters were recognized along Laboy river during the present survey (Fig. II–1–13).

1–7–1 Indications of Hot Spring Activity

Among the hot springs inside the Acupan Mine, those around Balatoc plug show higher temperatures and discharge rate than those outside the plug. Hot spring activity is most striking at the intersection of gold bearing veins and fracture zones at the margin of the plug.

Near Itogon bridge, hot water springs flow along irregular and discontinuous small fissures within a small plug similar to Balatoc. But, as the flow rate decreases during the dry season, it is considered to be related with ground water circulation.

The Dalupirip hot spring emanates from terrace deposite; the nature of the original host rock is unknown. However, judging from the geology of Dalupirip area, the spring waters may be coming from the interstratified paraschists and non-metamorphics that constitute the Pugo formation. Spring waters occurring on the other side of the river (left bank of Agno River) are cold.

The hot spring along Laboy river, ooze from the intersection of small fissures (E–W strike, 10 – 20 S dip) in the Itogon quartz diorite body. A NW–SE fault, associated with fracture zones, 5 – 6 m wide, occurs adjacent to the hot springs. As hot springs also occur at the southern end of this fault, both the Dalupirip and Laboy river hot springs may be considered to be associated with this NW–SE or NNW–SSE fault system.

1–7–2 Alteration Zones (Fig. II–1–13)

The alterations observed in the area are argillization and silicification. Green alteration related to burial diagenesis is observed in Pugo, Zigzag and Klondyke formations.

Alteration zones observed in relation with hydrothermal activity occur in the subsiding block in the Eastern part of the surveyed area. Among these zones, the white argillized zone (with sericite in the central part) occurring in the upper part of Laboy River, is associated with porphyry copper deposits, and thus considered to be related with the copper mineralization. The alterations occurring East of Baguio City show the following zonal structure: sericite – quartz (locally wairakite) zone, centered on the andesite porphyry-diorite porphyry complex, quartz-alunite (locally goethite) zone and (3) montmorillonite. Present day hot spring activity is observed associated with the gold deposits (Baguio Gold Mine and Baco Kelly Mine) located in the central sericite-quartz zone and with low grade mineralization in the quartz alunite zone. It is therefore considered that the observed zonation pattern is associated with the gold-silver deposits of ancient hot springs. There is no large scale zonation of the alteration minerals (sericite, quartz montmorillonite) in the alteration zones around Acupan-Itogon. Gold mineralization and hot water activity are observed in this area; it is considered that this gold-silver mineralization brought by circulation of thermal solutions is still going on.

1–8 Discharge Rates and Chemical Analyses of Rivers (Hydrological Survey)

The survey was carried out during the wet season. The discharge rates were measured and stream water samples were taken even during rainy days of the survey.

The discharge rate was measured by means of a short-type notch for a small creek flowing out from Dalupirip hot spring, and by means of a Price current meter for twenty other measurement points. Among these 21 measurement points, stream water samples from 11 points (1 to 11) were chemically analyzed (Fig. II–1–13, Table II–1–17).

However, in view of the bad weather conditions (rain and typhoon) during the time of measurement and sampling, the discharge rate and chemical analysis at a given place changed rapidly with time, and the interpretation of the data is rendered difficult.

Table II–1–6 Chemical Component of Running Water

Sample No.	Sampling site	pH	TDS	Acidity epm (pH4.8)	Alkalinity epm (pH8.3)	B	solv. Fe	Total Fe	Mn	As	Mg	Ca	Cℓ	SO_4	SiO_2	K	Na	HCO_3
1	DALUPIRIP	6.76	125	1.04	0.16	0.1	0.06	0.46	0.04	0.000	5.69	33.3	6.57	20.6	10.0	1.4	17.5	63.
2	TWIN RIVER	6.78	600	1.40	0.20	0.3	0.11	1.31	0.22	0.018	12.25	121.8	11.29	144.1	14.5	4.8	29.0	85.74
3	ITOGON RIVER	6.61	770	1.06	0.20	0.5	0.15	1.98	0.34	0.017	15.80	139.7	15.81	184.4	17.5	5.6	30.5	64.92
4	BARATOC	6.66	470	0.78	0.20	0.4	0.15	1.99	0.16	0.012	20.91	103.4	13.35	135.4	17.0	4.6	23.5	47.78
5	ACUPAN	6.78	395	1.52	0.20	0.0	1.12	1.10	0.16	0.001	31.61	75.4	4.11	76.4	14.0	2.0	14.0	93.09
6	PUGO BRIDGE	6.76	205	1.32	0.20	0.0	0.03	0.36	0.02	0.000	18.48	56.9	3.49	54.3	7.0	2.4	13.0	80.84
7	AMBUKLAO #2	6.95	80	1.52	0.20	0.0	0.01	0.06	0.01	0.001	23.82	19.2	3.70	11.3	12.0	0.4	16.0	93.09
8	LABOY BRIDGE	6.96	175	1.64	0.24	0.0	0.02	0.32	0.02	0.000	27.71	48.1	2.46	35.2	8.0	0.8	19.0	100.44
9	BACO – KELLY 1	3.36	415	0.00	1.26	0.0	0.38	0.76	0.72	0.000	23.34	52.9	9.86	116.7	21.0	1.6	18.0	0.00
10	BACO – KELLY 2	6.60	195	0.36	0.20	0.0	0.21	1.11	0.02	0.000	29.87	33.7	4.11	6.	20.0	1.2	16.5	22.05
11	BACO – KELLY 3	4.38	335	0.00	0.46	0.0	0.43	2.30	0.55	0.000	21.39	49.7	4.11	97.3	25.0	1.8	21.0	0.00

CHAPTER 2
GEOCHEMICAL EXPLORATION

CHAPTER 2 GEOCHEMICAL EXPLORATION

2–1 Purpose and Method of the Geochemical Exploration

This field survey is a preliminary exploration in preparation for a more detailed survey to be carried out in the future. Its purpose is to test several methods of geochemical exploration, and to check their validity. Being mainly methodological, this survey does not attempt to evaluate the geothermal reservoir occuring in the investigated area. The following techniques have been tested during the present survey:

1. Temperature measurement in soil at 1 m-depth (50 points),
2. Measurement of carbon dioxide gas concentration in soil gas (50 points),
3. Measurement of radon gas concentration in soil gas (50 points),
4. Measurement of mercury content in soil (50 points),
5. Measurement of mercury content of altered and unaltered rocks (40 samples),
6. Chemical analyses of hot-spring waters (10 samples),
7. Isotopic compositions (O and H) of hot-spring waters (12 samples),
8. Analyses of fumarolic gases (4 samples).

2–2 Geochemical Exploration at 1 Meter Depth

Soil temperature, CO_2 and Rn concentration in soil air, and mercury concentration in soil have been measured at 50 locations, principally along the roads of the investigated area. The distance between two locations is about 500 meters. The following results have been obtained.

2–2–1 Temperature Measurement at 1 Meter Depth

Temperature is measured by means of a Takara thermistor (Type A500) at the bottom of a one meter hole drilled by a hand auger (Fig. II–2–1.) The results are shown in Table II–2–1.

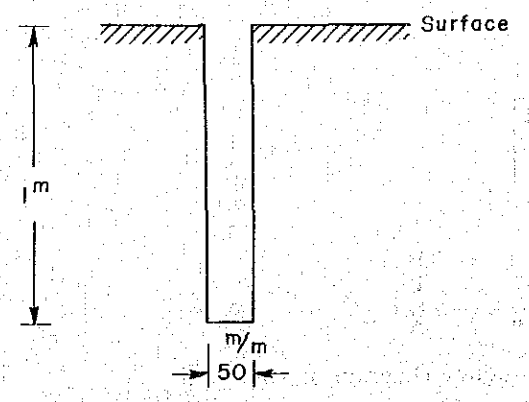

Fig. II–2–1 Profile of Hole for Temperature Measurement

As the survey lasted only a short period of time, there is no need for time correction.

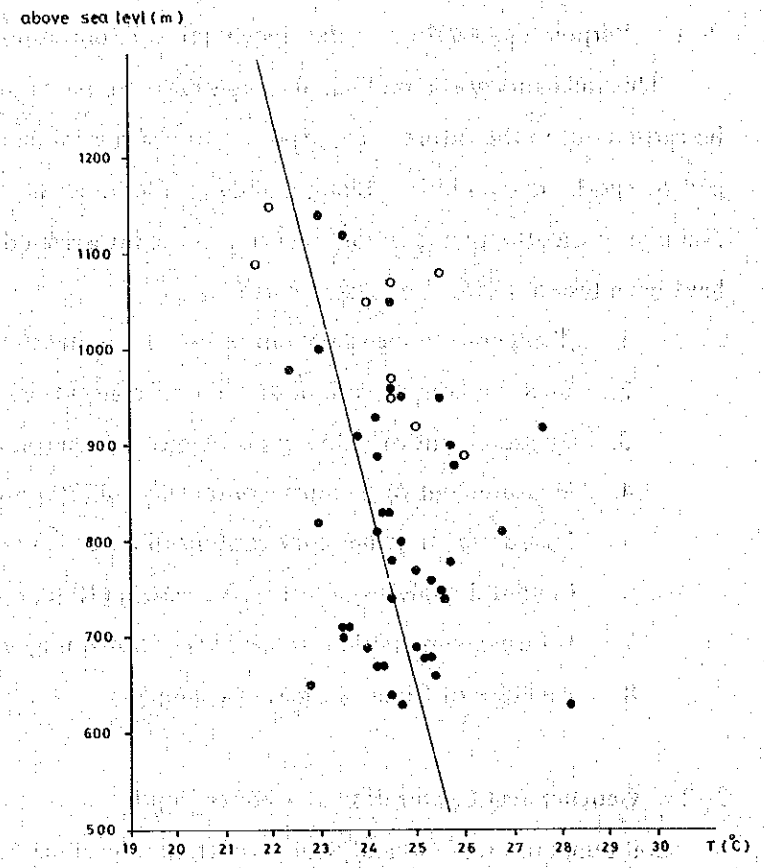

Fig. II–2–2 1m Depth Temperature-Sea Level Correlation

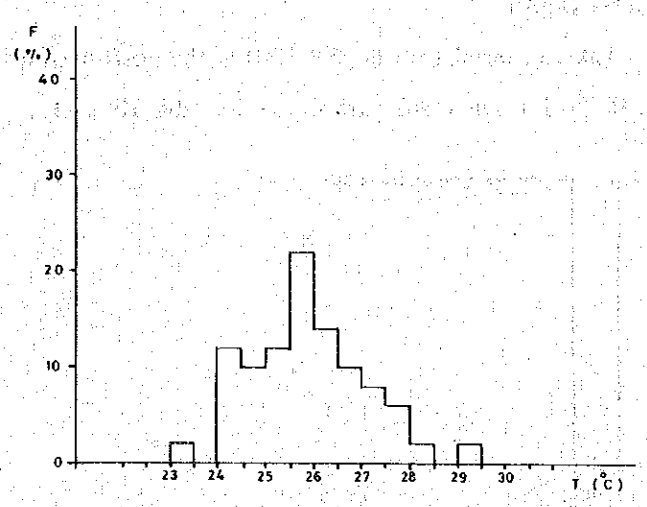

Fig. II–2–3 Frequency Diagram of 1m Depth Temperature Converted to 600m A.S.L.

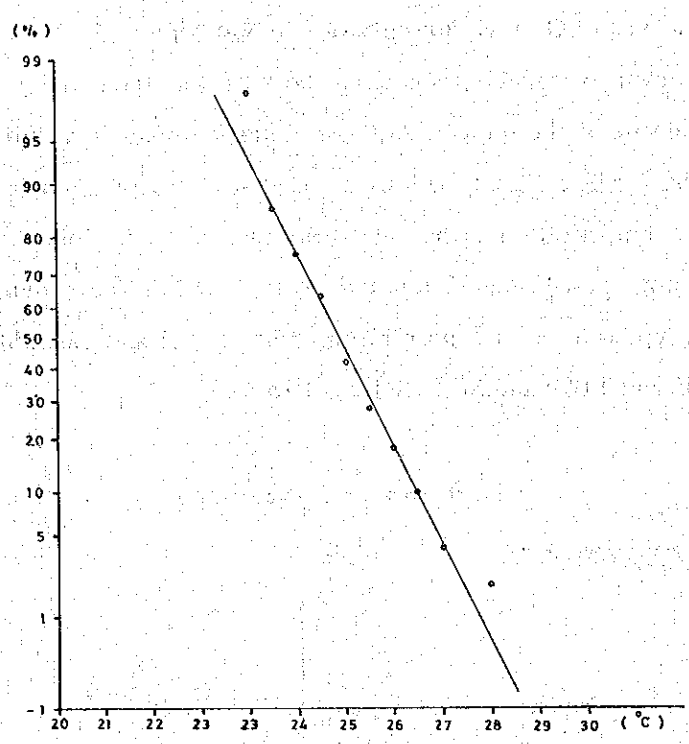

Fig. II–2–4 Probability Plot of 1m Depth Temperature Converted to 600m A.S.L.

The relationship between soil temperature and elevation in a.s.l. at each point is shown in Fig. II–2–2. The lowest and highest elevations in the investigated area are 630 m and 1,150 m, respectively. A negative correlation appears between temperature and elevation but it is not easy to draw a correlation line, the number of measurements being low and the dispersion high. The line drawn in Fig II–2–2 yields a correction factor of 2.5°C per 500 m of elevation, which closely agrees with the correction factors of 2.3°C per 500 m measured in Japan in July.
The frequency diagram and the probability plot of ground temperatures after applying the correction factor are shown in Fig. II–2–3 and II–2–4. The mean soil temperature ($\bar{x}$) at 600 m is 25.8°C, the standard deviation (v) is 1.2°C. Both show a relatively regular trend. The map of the soil temperature (Fig. II–2–5) is drawn according to $\bar{x}$, $\bar{x}$±v and $\bar{x}$+2v divisions. x+2v, x+v anomalies appear at Acupan Mine. Small scale anomalies of $\bar{x}$+v or more appear also at Virac and to the north. No positive geothermal anomaly appears along the road in the hot spring area of Itogon bridge. The soil temperature in this area is similar with the mean temperature of the whole area. The survey area may, thus, be divided into a southwestern part with high soil temperature, and a northeastern part with low soil temperatures.

2–2–2 Measurement of CO_2 Gas Concentration in Soil Air

The apparatus used for collecting soil gas is shown in Fig. II–2–6.

After measurement of the temperature, the atmospheric air is withdrawn from the hole using a double mouth syringe. The tube is then sealed at the top end and left to equilibrate for 24 hours. The CO_2 concentration in the soil gas is measured on the following day using a Kitagawa type gas detector. Three types of tubes are used for the detection depending on the gas concentration. SA type is used for concentrations between 0.1 and 2.6%; SB type for measurements between 0.05 and 1.0%; and SH type from 1 to 20%.

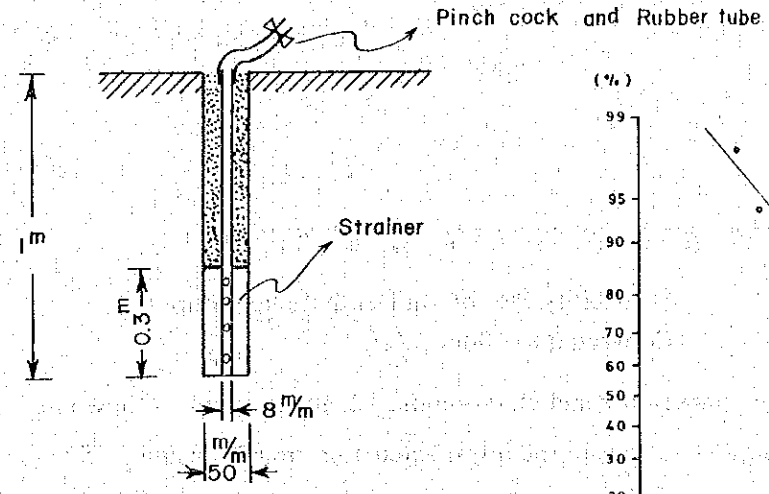

Fig. II–2–6 Collection of Soil Air

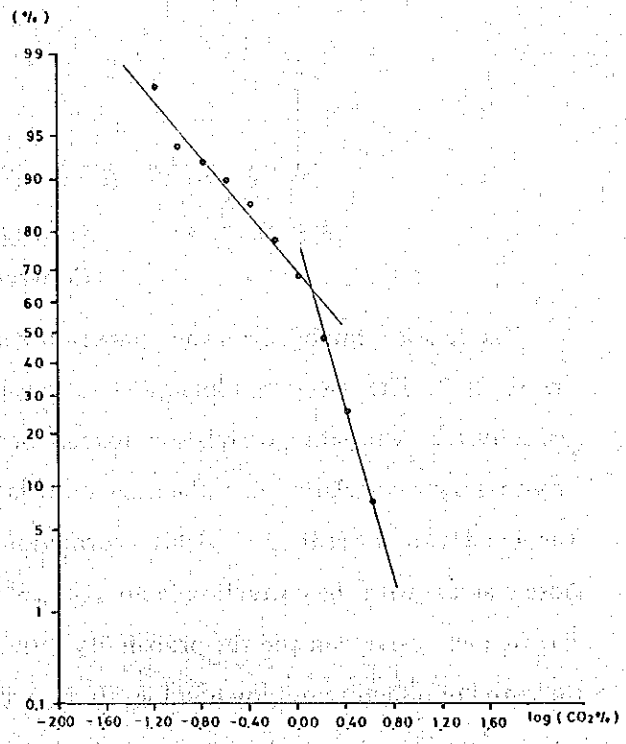

Fig. II–2–8 Probability Plot of CO_2 Gas Concentration

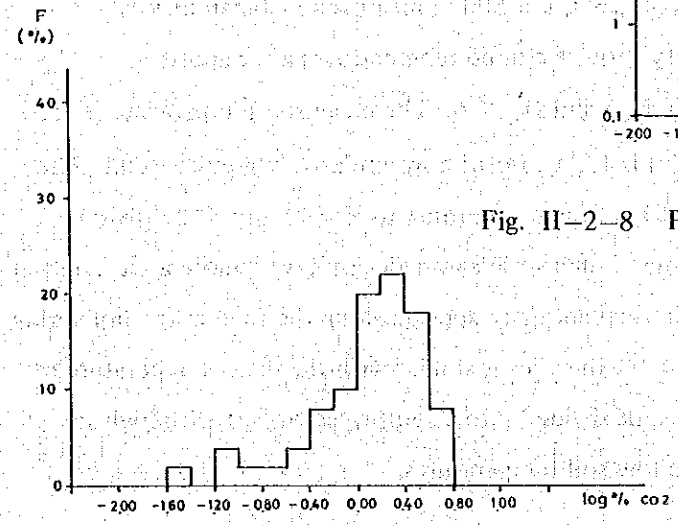

Fig. II–2–7 Frequency Diagram of CO_2 Gas Concentration

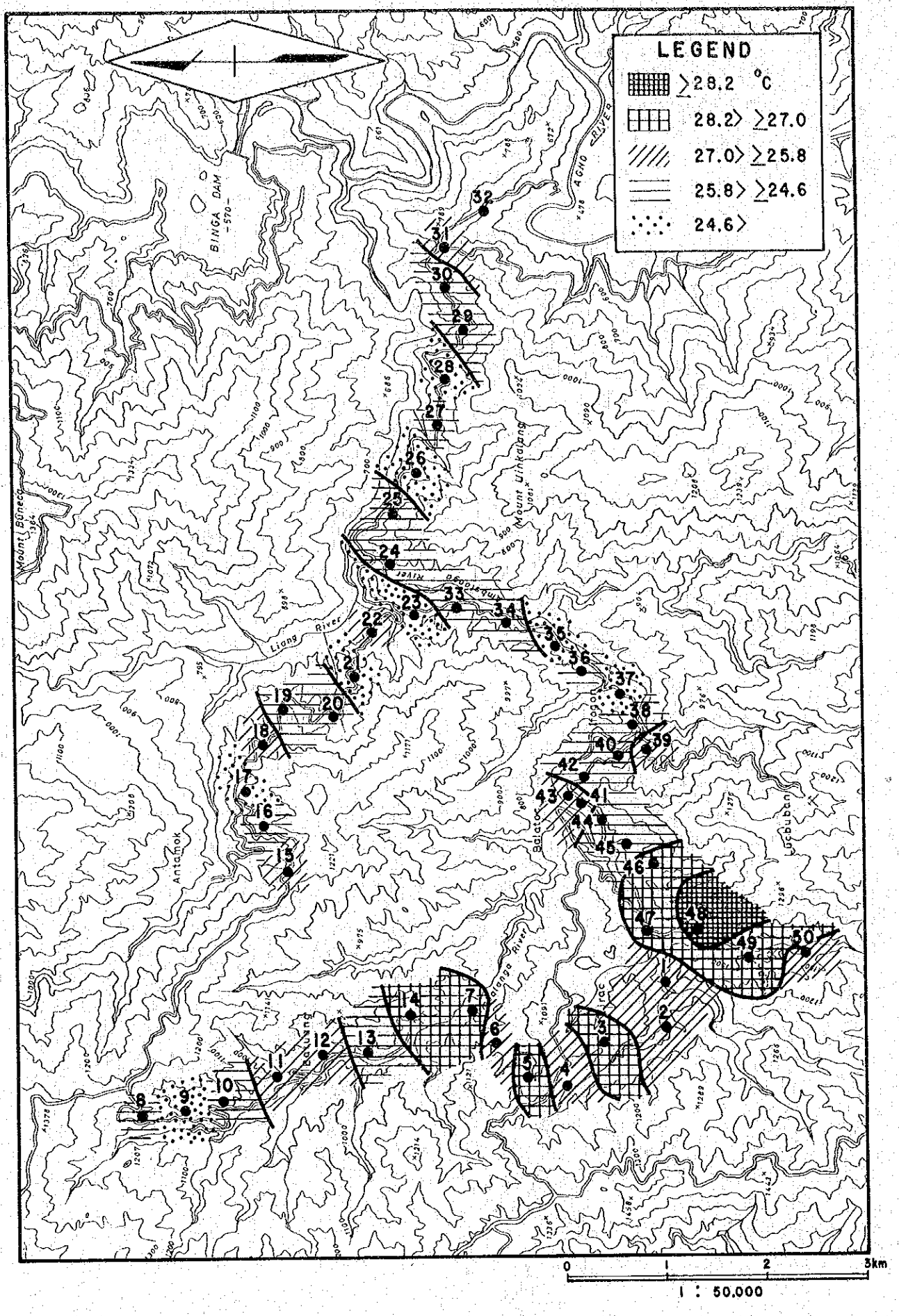

Fig. II–2–5 Distribution Map of 1m Depth Temperature Converted to 600m A.S.L.

Table II–2–1 Geochemical Data Sheet for 1m Depth Measurements

Point No.	Date Planting			CO_2 gas measurement		Track Etch Cup				Soil Colour	Geology	Elevation	Results			
	Date	Time	Ambient	Date	Time	Date Rec.	Exp. Days	Cup No.	Remarks				Hg	CO_2	Rn	T
			(°C)									(m)	(ppb)	(%)	(N/mm²30)	(°C)
1	13, Sep.	9:45	28.0	14, Sep.	9:40	7, Oct.	24	57581		dark brown	bio-hb-qtz diorite	920	320	0.09	12.2	25.0
2	"	10:50	32.0	"	10:20	"	"	57582		"	"	970	132	0.31	26.7	24.5
3	"	12:40	30.0	"	11:00	"	"	57583		"	lapilli tuff (Klondyke Fm.)	1080	4385	5.3	67.3	25.5
4	"	13.40	28.0	"	11:40	"	"	57584		brown	"	1070	67	1.6	26.0	24.5
5	14, Sep.	13.30	30.5	15, Sep.	8:45	"	23	57585	disturbed	reddish brown	"	1050	44	1.8	22.6	25.0
6	"	14:35	28.5	"	9:20	"	"	57586	dirty	dark brown	"	950	44	4.0	71.0	24.5
7	"	15:30	29.5	"	10.15	"	"	57587	"	reddish brown	"	890	35	3.3	24.9	26.0
8	15, Sep.	7:50	20.5	16, Sep.	10:18	12, Oct.	27	57588	"	brown	volc-plutonic complex	1150	39	2.25	45.0	22.0
9	"	8:40	20.0	"	9:41	"	"	57589		dark brown	"	1090	35	1.58	25.7	21.7
10	"	9:45	21.7	"	9:23	"	"	57590	dirty	brown	"	1000	53	2.75	83.7	23.0
11	"	10:40	27.7	"	8:55	"	"	57591	"	reddish brown	"	960	76	3.5	82.7	24.5
12	"	11:25	31.7	"	8:35	"	"	57592			"	930	44	1.95	264.0	24.2
13	"	12:50	28.5	"	8:05	"	"	57593		dark brown	"	890	48	1.65	170.6	24.2
14	"	13:45	26.3	"	7:35	"	"	57594		reddish brown	lapilli tuff (Klondyke Fm)	900	95	4.0	96.5	25.7
15	16, Sep.	7:15	24.3	17, Sep.	8:00	9, Oct.	23	57595		yellow orange	px. andesite por.	1120	25	0.72	21.1	23.5
16	"	7:50	21.0	"	8:55	"	"	57596		yellow orange	"	1140	30	1.05	12.0	23.0
17	"	8:35	22.4	"	8:30	"	"	57597	distroyed	brown	hb-qtz diorite	980	25	4.0	9.0	22.4
18	"	9:10	30.3	"	9:20	"	"	57598		light gray	"	950	9	1.7	6.0	24.7
19	"	10:05	30.3	"	9:40	"	"	57599		light brown	"	910	612	0.8	24.1	23.8
20	"	10:40	29.3	"	9:55	"	"	57600		brown	"	830	25	2.0	30.2	24.3
21	"	12:45	25.2	"	10:20	"	"	57601	dirty	"	"	820	98	1.85	24.1	23.0
22	"	13.25	30.0	"	10:40	"	"	57602		light brown	"	750	10	0.3	15.8	25.5
23	"	13:55	27.0	"	11:00	"	"	57603	dirty	yellow orange	"	710	83	1.38	55.1	23.6
24		14:30	29.7	"	7:10	"	"	57604		black	chlo-amphi schist (Pre-Tertiary)	640	44	0.68	6.7	24.5
25	17, Sep.	7:30	25.0	18, Sep.	7:30	"	22	57605		"	"	660	46	1.1	4.7	25.4

Point No.	Date Planting			CO_2 gas measurement		Track Etch Cup				Soil Colour	Geology	Elevation	Results			
	Date	Time	Ambient	Date	Time	Date Rec.	Exp. Days	Cup No.	Remarks				Hg	CO_2	Rn	T
			(°C)									(m)	(ppb)	(%)	($N/mm^2$30)	(°C)
26	17, Sep.	8:15	22.0	18, Sep.	7:55	9, Oct.	22	57606	dirty	dark brown	chlo-amphi schist (Pre-Tertiary)	650	271	0.63	13.3	22.8
27	"	9:10	23.8	"	8:20	"	"	57607	"	light brown	"	670	17	3.8	9.4	24.3
28	"	9:50	25.7	"	8:40	"	"	57608		black	meta-volcanics (Pugo Fm.)	690	98	1.1	2.3	24.0
29	"	10:40	27.7	"	9:00	"	"	57609	dirty	"	"	680	34	1.8	11.8	24.7
30	"	11:50	29.7	"	9:20	"	"	57610		"	"	680	78	3.4	11.0	25.3
31	"	13:15	28.5	"	9:45	"	"	57611	dirty	brown	hb-qtz diorite	740	39	1.38	22.0	25.6
32	"	14:05	36.0	"	10:15	"	"	57612		black	meta-volcanics (Pugo Fm.)	630	15	0.13	19.7	28.2
33	20, Sep.	7:45	22.5	21, Sep.	7:55	"	19	57613	ant. infested	yellow orange	hb-qtz diorite	680	15	1.18	13.6	25.2
34	"	8:20	23.3	"	8:15	8, Oct.	18	57614		brown	"	670	22	4.55	50.1	24.2
35	"	8:55	22.8	"	8:20	"	"	57615	dirty	"	"	700	32	0.75	23.1	23.5
36	"	9:30	23.0	"	8:50	"	"	57616	"	dark brown	"	690	10	2.35	22.1	25.0
37	"	10:05	24.0	"	9:05	"	"	57617	"	light brown	"	710	10	0.98	15.3	23.5
38	"	10:45	24.8	"	9:22	"	"	57618	"	brown	"	740	756	0.54	6.7	24.5
39	"	11:40	23.0	"	9:40	"	"	57619		light brown	andesitic volcanics (Zi.Em Fm.)	760	50	5.90	29.8	25.3
40	"	13:00	25.2	"	10:05	"	"	57620	dirty	brown	dacitic breccia pipe	780	780	1.90	14.4	24.5
41	"	13:45	22.2	"	10:25	"	"	57621	disturbed	yellow orange	lapilli tuff (Klondyke Fm.)	810	228	2.80	26.0	24.2
42	"	15:25	21.5	"	10:45	"	"	57623	"	dark brown	"	780	705	4.2	21.1	25.7
43	"	15:25	25.5	"	8:05	"	"	57622	"	reddish brown	"	770	619	1.6	19.2	25.0
44	"	15:00	26.5	"	8:25	"	"	57624	dirty	black	"	800	1720	2.5	50.1	24.7
45	"	14:00	27.5	"	8:45	"	"	57625	"	yellow	"	830	381	0.45	22.1	24.4
46	"	13:30	24.5	"	9:00	"	"	67626		light brown	andesitic volcanics (Zi.Em Fm.)	880	153	1.5	38.5	25.8
47	"	11:30	29.0	"	9:30	"	"	57627	dirty	orange	bio-hb qtz diorite	810	40	0.49	34.7	26.8
48	"	10:15	26.5	"	9:50	"	"	57628		brown yellow	andesitic volcanics (Zi.Em Fm.)	920	123	0.75	51.1	27.6
49	"	9:15	28.0	"	10:20	"	"	57629		dark black	"	950	1596	0.20	15.3	25.5
50	"	8:20	24.5	"	10:55	"	"	57630		brown	"	1050	1262	0.03	18.2	24.5

The results are shown in Table II–2–1. Fig. II–2–7 and II–2–8 are the frequency diagram and the probability plot of the logarithms of CO_2 concentration in soil air. The mean value ($\bar{x}$) and standard deviation (v) of Log CO_2% are 0.10 and 0.47 respectively. This mean value of 0.10 is similar with the threshold value deduced from the probability plot (Fig. II–2–8). Fig. II–2–9 is a map showing the distribution of CO_2 concentration according to divisions along $\bar{x}$, $\bar{x} \pm v$ and $\bar{x} - 2v$. The CO_2 concentration is extremely low in the west of Acupan Mine, and high in the vicinity of the Itogon Bridge hot spring area. High concentrations are spotty and there is no regularity in the distribution of CO_2 values. There is also no correlation with the soil colour, nor with the soil thickness, which is generally extremely poor in this area.